UiT
THE ARCTIC
UNIVERSITY
OF NORWAY

Faculty of Science and Technology
Department of Physics and Technology

An evaluation of the reanalyses ERA-Interim and ERA5 in the Arctic using N-ICE2015 data

—

Liv-Ellen Fredriksen

EOM-3901 Master thesis in Energy, Climate and Environment – June 2018

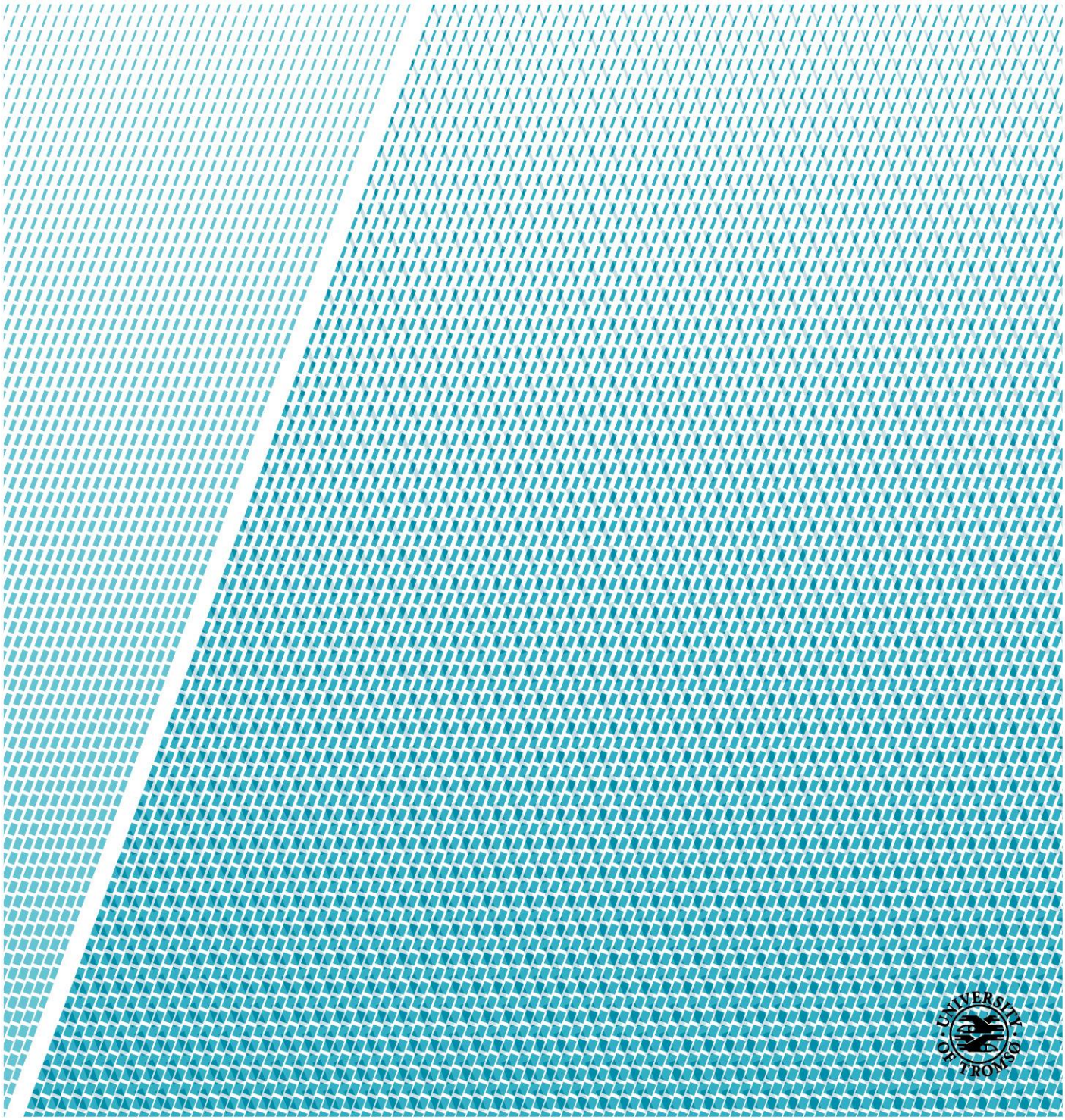

Abstract

The Arctic climate has changed considerably in the last few decades. Hence, a large fraction of the current studies of the Arctic climate relies on global atmospheric reanalyses, due to the shortage of meteorological observations in the Arctic. However, global climate models have shown to struggle with simulating the current conditions in the Arctic region. Thus, the objective of this thesis is to evaluate how accurate the reanalysis ERA-Interim and ERA5 are in representing the measurements from the Norwegian Young Sea Ice (N-ICE2015) expedition obtained in 2015 North for Svalbard. The observations from N-ICE2015 are a good data set for using in the evaluation. The reason for this is due to the fact that N-ICE2015 provide measurements obtained over the thinner sea ice condition in the Arctic during the winter season, which no other Arctic expedition can provide. Moreover, the ERA5 reanalysis is newest reanalysis produced and few studies have evaluated on ERA5's performance in the Arctic.

In addition, the thesis will focus on how the assimilated N-ICE2015 observations affect the reanalyses ERA-Interim and ERA5. Final objective is to see if new reanalysis ERA5 shows improvements relative to ERA-Interim representing the previous reanalysis generation.

The results found in the thesis confirmed that the assimilated observations from N-ICE2015 have influenced both reanalyses ERA-Interim and ERA5. Furthermore, both reanalyses overestimate the near surface temperature during the whole period when N-ICE2015 took place. In addition, the biases found for the downward- / upward- shortwave radiation and net shortwave radiation suggest that both reanalyses have a too low surface albedo and present erroneous cloud conditions.

Acknowledgments

First and foremost, I wish to thank my supervisor at NPI – Norwegian Polar Institute, Robert M. Graham. His guidance, encouragement and support have been in invaluable to me during this period. He has shown support in a number of ways, starting with guiding how to start working on the thesis, recommendation of relevant articles, assisting whenever needed for the data collections and presenting the results, feedbacks and explanations on results and progress made during our almost weekly meeting these few months. My thanks will also go to NPI for providing the N-ICE2015 data used in this thesis.

I would also like to thank my supervisor at UiT – The Arctic University of Norway, prof. Rune Graversen, for the dozen times he had to explain to me how the reanalyses worked and discussion of the result found have helped me to develop an understanding of the subject. In addition, I would like to thank him for proof reading the thesis and fast replying of the feedbacks.

Finally, I want to express gratitude to my family for the support and encouragement during this period. Especially, my big brother Arnt deserves recognition for his assistance whenever I got stuck and for proofreading this thesis.

Abbreviations

ASCOS	Arctic Summer Cloud-Ocean Study
AVHRR	Advanced VHRR
DEWLINE	Distant Early Warning
DMSP	Defence Meteorological Satellite Program
ECMWF	European Centre for Medium-Range Weather Forecasts
ERA-I	ERA-Interim
FGGE	First GARP Global Experiment
IFS	Integrated Forecast System
IPY	International Polar Year
LW	Longwave radiation
LWD	Downward longwave radiation
LWN	Net longwave radiation
LWU	Upward longwave radiation
MSLP	Mean sea level pressure
N-ICE2015	The Norwegian Young Sea Ice
NOAA	National Oceanographic and Atmospheric Administration
QVI	Vertically integrated water vapour (water vapour path)
SHEBA	Surface Heat Budget of the Arctic Ocean
SW	Shortwave radiation
SWD	Downward shortwave radiation
SWN	Net shortwave radiation
SWU	Upward shortwave radiation

T2m	2m temperature (near-surface temperature)
TIROS	Television Infrared Observation Satellite
TOVS	TIROS Operational Vertical Spectrometer
VHRR	Very High-Resolution Radiometer
U10M	Total wind speed
U10m	East-West wind speed
V10m	North-South wind speed

Table of Contents

List of Tables

List of Figures

1 Introduction

The Arctic climate has changed a lot during the last decades. Noticeably, the Arctic region has been leading focus of many climate change studies in the recent years, but the curiosity for the Arctic region has been there for centuries.

The interest in the Arctic region started in the sixteenth century when nations of northern Europe saw this as a potential route to China [*Serreze and Barry, 2014*]. Nevertheless, over two hundred years later the modern basis of Arctic science and meteorology emerged when Karl Weypricht's suggested in 1875 a need for International Polar Expedition. The First International Polar Year (IPY) was arranged during the period 1882-1883 a few years after Karl Weypricht had died. During the first IPY twelve principle stations were established in the North Polar Region, and a detailed account of various national expeditions is provided by [*Barr, 1985*]. A decade later from September 1893 through August 1896 the Norwegian vessel *Fram* drifted across the Arctic Ocean from New Siberian Islands to Spitzbergen [*Nansen, 1898*]. This was a bold new direction in Arctic explorations, because of previous expeditions tragic endings (e.g. shipwreck, stuck due to bad weather). Different to other previous expedition Nansen used a specially designed vessel that could be lifted up by the ice, and drift with the ice. The success from this voyage gave a massive knowledge of ice motion and Arctic Ocean circulation.

The strategic importance of the Arctic seas was demonstrated in World War II (1940-1945), when Germany established secret weather stations in East Greenland and Spitzbergen. The same concept was later used by America and Soviet Union during the Cold War. The U.S and Canadian governments established a few weather stations in the Canadian Arctic Archipelago, and later initiated the Distant Early Warning LINE (DEWLINE) for the intent to warning of nuclear attack from Soviet Union. On the other hand, the Soviet Union started up with their North Pole drifting station program, and the latest drifting station was built in 2015 [*Russian North Pole drifting station program, www.arctic.ru*].

Later, in the early 1970s started satellite based observations of the Arctic regions. In addition, a few Arctic expeditions have occurred the past two decades. A few of this expedition lasted for a whole year such as SHEBA [*Perovich et al., 1999*], Russian North Pole drifting stations

[*Kahl et al., 1999*] and Tara [*Gascard et al., 2008; Vihma et al., 2008*], while others have only occurred during the summer time ASCOS [*Tjernström et al., 2013*] and CEAREX [*CEAREX Drift Group, 1990*]. In addition, one of the latest Arctic expedition is The Norwegian Young Sea Ice (N-ICE2015) [*Cohen et al., 2017*] that occurred during the winter season. A few of this Arctic field campaigns will be explained more later in the thesis. It is worth to mention that observations from a few of these Arctic expeditions and satellite data are assimilated into various numerical weather prediction models.

A simple definition of data assimilation is that a person can think of it as the most favourable merging of models and observations. Moreover, data assimilation is the main element of numerical weather prediction. A few of these numerical weather predictions cover the whole globe and they are called global atmospheric reanalyses. Atmospheric reanalyses provide gridded analyses that covers many years of atmospheric humidity, winds, temperature, pressure heights, and other variables. These data are provided from historical observations from satellites, radiosondes, collected during expeditions and other sources are assimilated into a numerical weather model. In addition, the atmospheric reanalyses provide forecasts for different variable such as precipitation.

In the recent decades the Arctic has changed a great deal, and this change has caused more interest for studying the climate in the Arctic. The warming in the Arctic has been at least twice as fast when compared to the lower latitudes [*Blunder and Arndt 2012]*. The decline in the sea ice cover is one of the most noticeable indicators of the Arctic warming [*Vihma et al., 2014*]. The decrease in sea ice extent and thickness, observed increase in the amount of open water for the recent decades and the lengthening of the melt season have been documented in many studies [e.g. *Comiso et al., 2008; Maslanik et al., 2011; Stroeve et al., 2014; Comiso et al., 2012; Johannessen et al., 1999*]. The change in the sea ice extent has been reasonably well documented since 1979, because of accessibility of satellite passive microwave remote sensing data. Consequently, communities have become aware of that many regions in the Arctic now experience seasonal ice coverage, and a larger area of the ice pack is made up of first-year ice [*Maslanik et al., 2011; Comiso et al., 2012; Nghiem et al., 2007*].

However, the extend of the Arctic sea ice cover is not only a noticeable indicator of the climate change. In addition, the Arctic sea ice has strong feedback effects on other components of the climate system [*Vihma et al., 2014*]. Consequently, due to the decline in sea ice cover, the surface 2-m air temperature (T2m) has increased [*Overland et al 2008*]. The

incline for the surface temperature in the Arctic is two to four times faster than the global average [*Bekryaev et al., 2010; Miller et al., 2010; Solomon et al., 2007*]. In addition, a study has shown that in the Arctic Ocean the strongest warming occurs in the coastal and archipelago surrounding this area [*Polyakov et al., 2012*].

The sea ice has two characteristics for affecting the other components of the climate system [*Vihma et al., 2014*].

a) Reduction of prevention in the exchange between the atmosphere and the ocean of e.g. heat, water vapour and momentum.
b) The sea ice has much higher surface albedo, than the open ocean.

Consequently, from point a) more heat will be lost from the ocean to the atmosphere, due to the reduction of insulation with the declining sea ice cover. In addition, the sea ice albedo feedback is one of the main processes driving "Arctic Amplification" [*Serreze and Barry, 2011*]. The "Arctic Amplification" define that greater warming occurs in the Arctic than globally.

Furthermore, the changing in sea ice causes increase of the moisture transport [*Woods et al., 2013*], due to the fact that the reduction of sea ice will increase local availability of moisture in the Arctic. In addition, the increase in moisture transport is due to the storms that occurs in the Arctic. Thus, heat and moisture are transported from lower latitudes. In addition, the strong winds related to the storms drive upper ocean mixing and sea ice drift [*Meyer et al., 2017; Itkin et al., 2017; Peterson et al., 2017*]. Moreover, the increase in moisture is important for the atmosphere due to feedback effects on longwave radiation from water vapor and clouds. A few studies have found that the increase in longwave radiation related to moisture transport from lower latitudes is an important process driving Arctic amplification [e.g. *Francis et al., 2005; Graversen and Wang, 2009; Kapsch et al., 2014; Park et al., 2015*]. The clouds brought from storms can have complicating effects on the Arctic climate [e.g. *Perovich et al., 2008; J. Zhang et al., 2008; Persson et al., 2016*]. One of the primary uncertainties in our understanding of the Arctic amplification is the Arctic clouds. Hence, they are quite an active area of research [e.g. *Kay and Gettelman, 2009; Persson et al., 2016*].

A large fraction of the current studies of the Arctic climate relies on global atmospheric reanalyses. In view of the fact that there so few observations in the Arctic, it is important find out how the atmospheric reanalyses present the Arctic climate. Therefore, this study's

objective is to see if the newest atmospheric reanalyses ERA5 and its predecessor ERA-Interim will give a good representation of the Arctic climate during the both winter and spring months by comparing with the measured N-ICE2015 data. In addition, this study will also check what impact the assimilation of N-ICE2015 observations into the reanalysis ERA-Interim and ERA5 have on the reanalyses.

2 The Arctic region

2.1 Other Arctic expeditions

This chapter focus will be about a few other Arctic expeditions. The reason for this is due to the fact that many of the studies used to compare with the results found in this study have used observations data from these expeditions.

2.1.1 ASCOS

During the International Polar Year (IPY), 2007-2008 the Swedish-led field experiment Arctic Summer Cloud-Ocean Study (ASCOS) was carried out from 1 August to 9 September 2008. The icebreaker *Oden* was moored to an ice floe for three weeks, drifting with the ice as seen in Figure 1. Study of the life cycle and formation of low-level Arctic clouds was the focus for ASCOS expedition [*Tjernström et al., 2012; Tjernström et al., 2014*]. Some of the data that were collected during the expedition comes from ship-mounted sensors in operation during the whole expedition. In addition, a few other measurements are only available from the ice drift period, due to the fact that they were obtained by using ice-deployed instruments.

An automated weather station was mounted onboard *Oden.* The machine obtained observation of basic meteorological quantities. Furthermore, during ASCOS 145 radiosondes were launched with a 6-hourly interval between each launch. However, into the ERA-Interim the 6-hourly surface pressure and wind observations from *Oden* were assimilated.

During the ice drift period, the observations obtained were all four components of the surface radiation budget (Long-\ Shortwave upward and downward radiation). In addition, measurements of the near-ice air temperature, humidity and wind speed were obtained from a mast on the ice. As well, from an eddy covariance method, using a combination of sonic

anemometers and fast open-path gas analyses, the turbulent fluxes of sensible and latent heat were estimated.

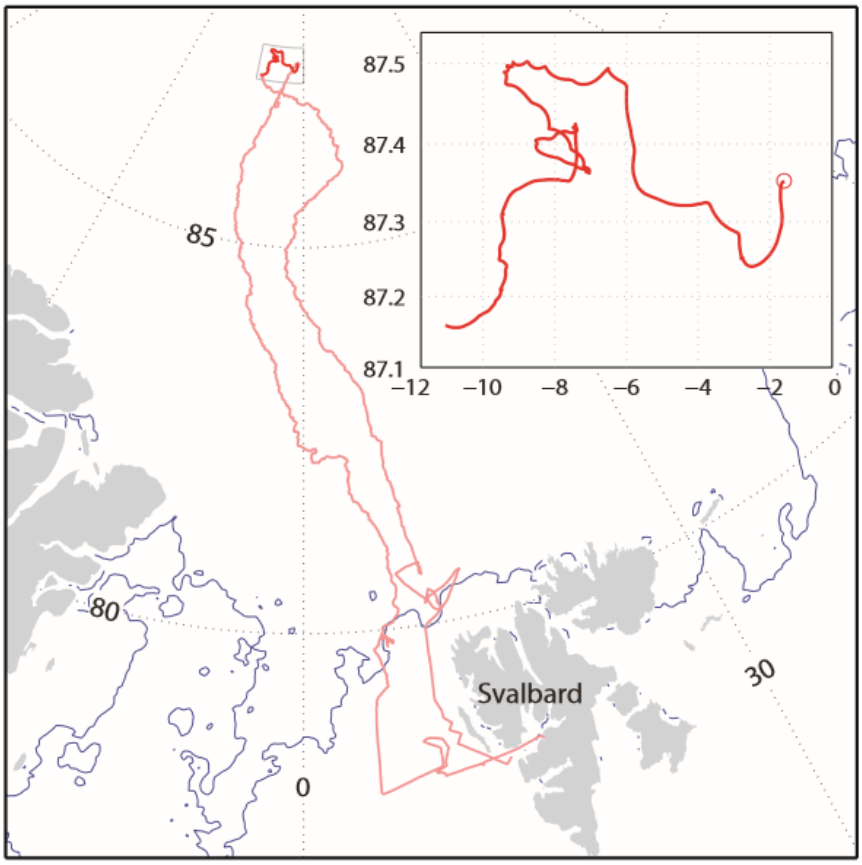

Figure 1: ASCOS drift from 2 August to 8 September 2008 [Wesslén et al., 2014]

2.1.2 TARA

Meteorological, oceanographic, and sea ice measurements were made during 2006-2007 at the drifting ice station Tara [*Gascard et al., 2008; Vihma et al., 2008*] seen in Figure 2. The expedition was a part of the European project DAMOCLES (Developing Arctic Modelling and Observation Capabilities for Long-Term Environmental Studies).

From 25 April to 31 August 2007 the drifting ice station Tara collected tethersonde sounding data on air humidity, air temperature and wind speed in the central Arctic. The data collected during this expedition were not assimilated into the reanalyses. During this period, a total of 95 tethersonde soundings through 39 sounding per days were made. The vertical profiles of relative humidity, the air temperature, wind direction up to the height of 2 km and wind speed were measured using a Vaisala DigiCORA Tethersonde System.

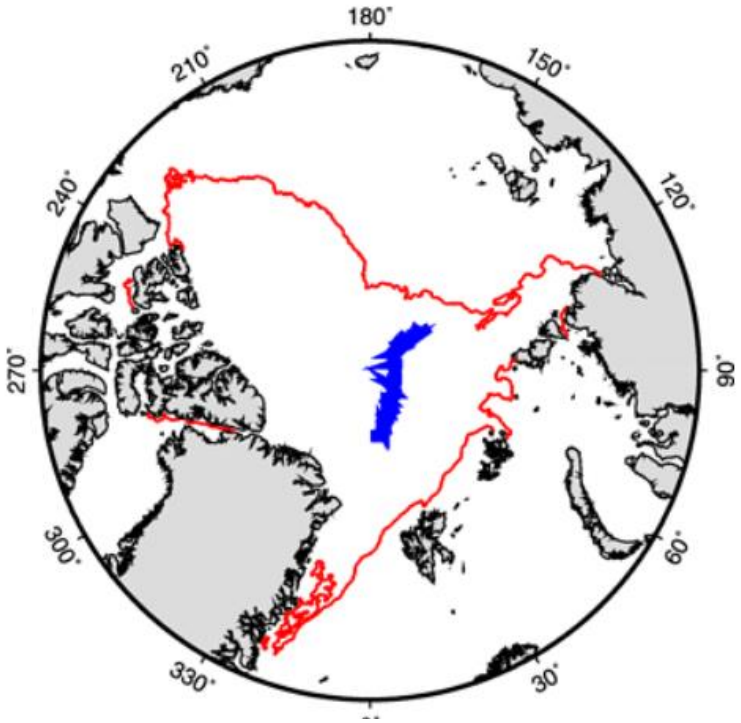

Figure 2: TARA drift track (in blue), from 25 April to 31 August 2007. Shown (in red) is the sea ice edge on 17 September 2007 [Jacobson et al., 2012].

2.1.3 SHEBA

In the Beaufort Sea, north of Alaska was the Surface Heat Budget of the Arctic Ocean (SHEBA) ice station in operation from 2 October 1997 to 11 October 1998 [*Perovich et al 1999*], and drifted 2800 km (Figure 3). SHEBA collected near continuous observation over a relatively thick multiyear ice floe.

The SHEBA near-surface temperature (T_{2m}) measurements were measured at a height of 2.5 m, as opposed to the more common measuring temperature at 2 m height. The measuring equipment were mounted on a 20 m high mast, that obtained the temperature and 10 m wind speed. For measuring the broadband longwave radiative heat flux, they used Eppley Precision Infrared Radiometer hemispheric flux pyrgeometers. Also, they launched GLASVaisala Rawinsondes two times each day that measured shortwave radiation [*Graham et al., 2017*].

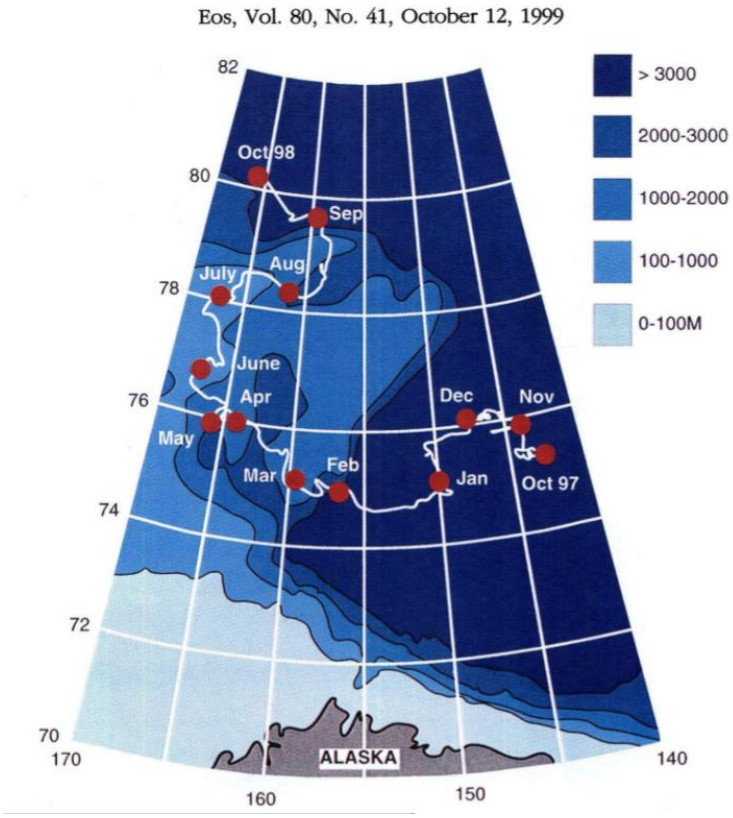

Figure 3: Drift track for SHEBA field campaign from October 1997 to October 1998. The start of each month is represented by the red dot. [Perovich et al., 1999]

2.2 Arctic meteorology

All of these expeditions described in previous section 2.1 have taken place at different regions in the Arctic. Furthermore, each region has its own climate depending on the different conditions. Correspondingly seen in Figure 4 the regions in the Arctic have different land and ocean cover. In addition, the place that the N-ICE2015 expedition took place have easy access to the Atlantic Ocean, which has a huge influence on the climate in this area. Very few observations have been taken in the North Atlantic region, where the N-ICE2015 expedition drifted. The other expeditions have mostly drifted even farther north than N-ICE2015 or in the seas over Alaska and Siberia.

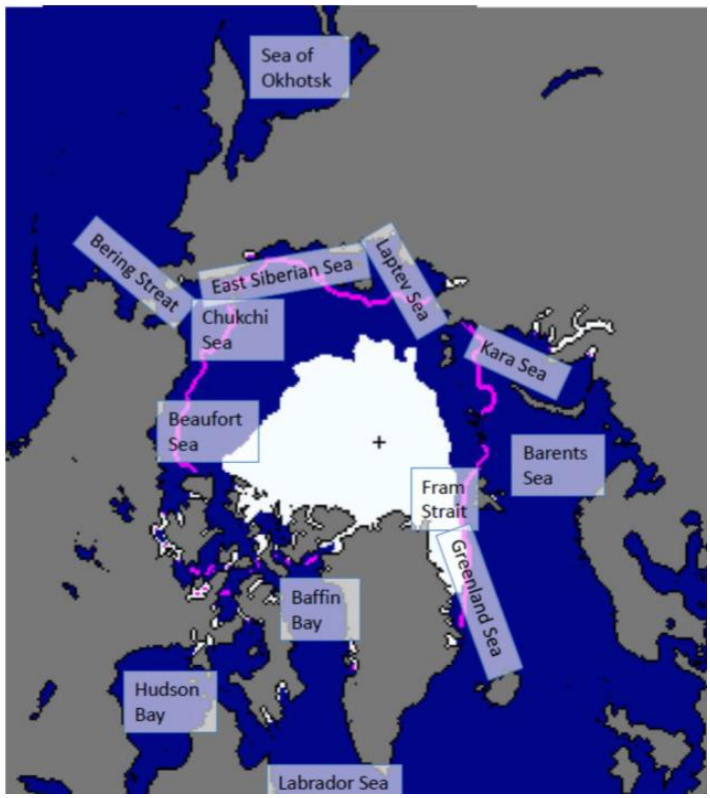

Figure 4: The Arctic region. The figure shows the Arctic sea ice extent in September 2012 (white area) compared with the median ice edge (purple line) in the period 1979 – 2012. The image is found in [Vihma et al., 2014].

These expeditions have had different focus on what they study of the Arctic meteorology. As mentioned before the ASCOS focus was to study the clouds in the Arctic region. Moreover, the expedition has provided new and unique observations of the Arctic. For the Arctic meteorology the results from ASCOS can improve the knowledge for low-level clouds in the summer central Arctic Ocean, as well as about their formation [*Tjernström et al., 2014*].

The data from the SHEBA have been a large help to shape our understanding of the Arctic climate, especially during the winter season where the quantity of observations are small [*Stramler et al., 2011*]. Furthermore, the data from SHEBA in the Pacific sector and data from N-ICE2015 in the Atlantic sector have disclosed that the Arctic climate operates in two unmistakeable winter states [*Stramler et al., 2011; Graham et al., 2017*]. The most usual winter state is characterized by cold surface temperature, strong surface inversion and a large negative (upward) net longwave radiation flux (LWN) at the surface [*Stramler et., 2011; Raddatz et al., 2015; Pithan et al., 2014*]. This winter state is called the "radiatively clear

state" [*Graham et al., 2017*]. The other state is the "opaquely cloudy state", which is characterized by higher surface temperature, LWN is approximately 0 $W\ m^{-2}$, and typically has lower surface pressure [*Stramler et al., 2011; Raddatz et al., 2015*].

In addition, other locations in the Arctic have observed the two Arctic winter states. For example, during the winter of 2007 – 2008 over the sea ice the Amundsen Gulf of the Canadian Arctic [*Raddatz et al., 2015*]. This location is near Beaufort Sea in Figure 4. In addition, the two winter states have been observed at land-based stations in Barrow, Alaska, and Eureka, Canada [*Cox et al., 2012*]. Due to these data over the sea ice, studies have found out that the two Arctic winter states are not a distinct feature for only a small part of the Arctic [*Graham et al., 2017*]. Moreover, analyses of satellite data have suggested that the two Arctic winter states are probable to operate over the larger part of the Arctic Basin [*Cesana et al., 2012; Stramler et al., 2011*].

2.3 Satellite observation in the Arctic

Satellite based observations of the Arctic regions started in the early 1970, when the National Oceanographic and Atmospheric Administration's (NOAA) and U.S Air Force Defence Meteorological Satellite Program (DMSP) system Television Infrared Observation Satellite (TIROS) provided useful analyses of the sea ice extend and cloud systems with the use of the Very High-Resolution Radiometer (VHRR).

Now there exists quite a lot of satellites that pass over the polar region more than once a day. Satellites are used to determine the temperature profiles, cloud height, surface albedo, moisture content and other variables for the climate. The satellites do not measure the temperature directly, but rather the heat radiation from the Earth's atmosphere. The heat radiation is then used to estimate the temperature profiles.

Satellite observations have been important for our insight into the Arctic meteorology and sea ice. This may be argued by the latest changes which have been observed in the Arctic sea ice [*Johannessen et al., 1999*]. It has been confirmed that during the period 1978 to 1998 with the use of microwave satellite remote sensing data, there has been a reduction of the area to the multiyear ice in the winter season. Furthermore, there has been a study of warming trends in the Arctic with the use of satellite thermal infrared data for surface temperatures with condition that it is cloudless [*Comiso et al., 2003*].

In the late 1970s the data from TIROS-N systems with Advanced VHRR (AVHRR), and the TIROS Operational Vertical Spectrometer (TOVS) were found widely used by the community. The data from TOVS are assimilated into various numerical weather prediction models. Satellite data from TOVS includes the following instruments listed below. Data values from this have been in usage in various models since ERA-40 [*Dee et al., 2011*].

- HIRS (High-resolution Infrared Spectrometer) – Delivers high-resolution temperature profile, but under the condition that it must be cloudless.
- MSU (Microwave Sounding Unit) – Measure the radiation in the atmosphere from the 1979. In 1998 came AMSU (Advanced Microwave Sounding Units) with higher accuracy as the successor for MSU.

- SSU (Stratospheric Sounding Unit) – From 1979 the SSU has been delivering a near global stratospheric temperature data above the lower stratosphere.

3 Methodology and Data Sources

3.1 N-ICE2015

The Norwegian Young Sea Ice (N-ICE2015) expedition took place from January to June in 2015 on the Norwegian Research Vessel, R/V *Lance*. The vessel was frozen into an ice pack north of Svalbard on 15 January, and then allowed to drift into the ice. During the expedition, the observations were taken over four separate ice drifts (Floes 1 to 4) seen in Figure 5. For Floes 1 and 2 (January-March) took place at 81-83.5N, 16-38E and Floes 3 and 4 (April-June) took place 80-83.5N, 3-16E [*Cohen et al.,* 2017]. When each floe was inhabited nearly continuous measurements for atmospheric, cryospheric, oceanic and biological were obtained.

The N-ICE2015 expedition had the focus on collecting meteorological data over the new thin sea ice, covering the seasonal change that occurs between January and June [*Cohen et al., 2017*]. Furthermore, a few problems did occur during the expedition. As seen from Figure 5, measurements were obtained from four different ice floes. The reason for this occurred due to the fact that it was not possible to deploy the instruments on the ice, when the floe had broken up.

From a 10m high mast temperature, wind and mean sea level pressure measurements were taken. The long wave radiative fluxes were obtained from a radiation station. The primary data from these measurements have a 1-minute resolution [*Cohen et al., 2017; Hudson et al., 2015*]. Also, radiosondes were launched from the ship two times each day, near 1100 and 2300 UTC [*Graham et al., 2017*]. From these radiosondes, the water vapor and 850 hPa temperature measurements were derived.

In this study, the atmospheric observations used are averaged to 6-hourly resolution. Generally, the N-ICE2015 expedition can be split into two nearly continuous periods [*Kayser et al., 2017*]. The first of two periods would cover the winter period from January to March and corresponds to the drifts of Floe 1 and Floe 2. The second period covers the spring period from April to June and corresponds to the drifts of Floe 3 and 4. More detailed description of the data and measuring instruments is found in Cohen et al., 2017.

The variables that will be used for the evaluation in this thesis are:

- Near surface temperature/ 2 m temperature: Temperature that is obtained at 2 meters height above surface.
- Mean sea level pressure: measurements obtained from a 10 meter mast that was set up on the ice floe
- Vertically integrated water vapor: Derived from balloon borne radiosonde data
- 10-meter wind speed: Wind speed that is measured 10 meters above the surface.
- Shortwave radiation (down, up and net)
- Longwave radiation (down, up and net)

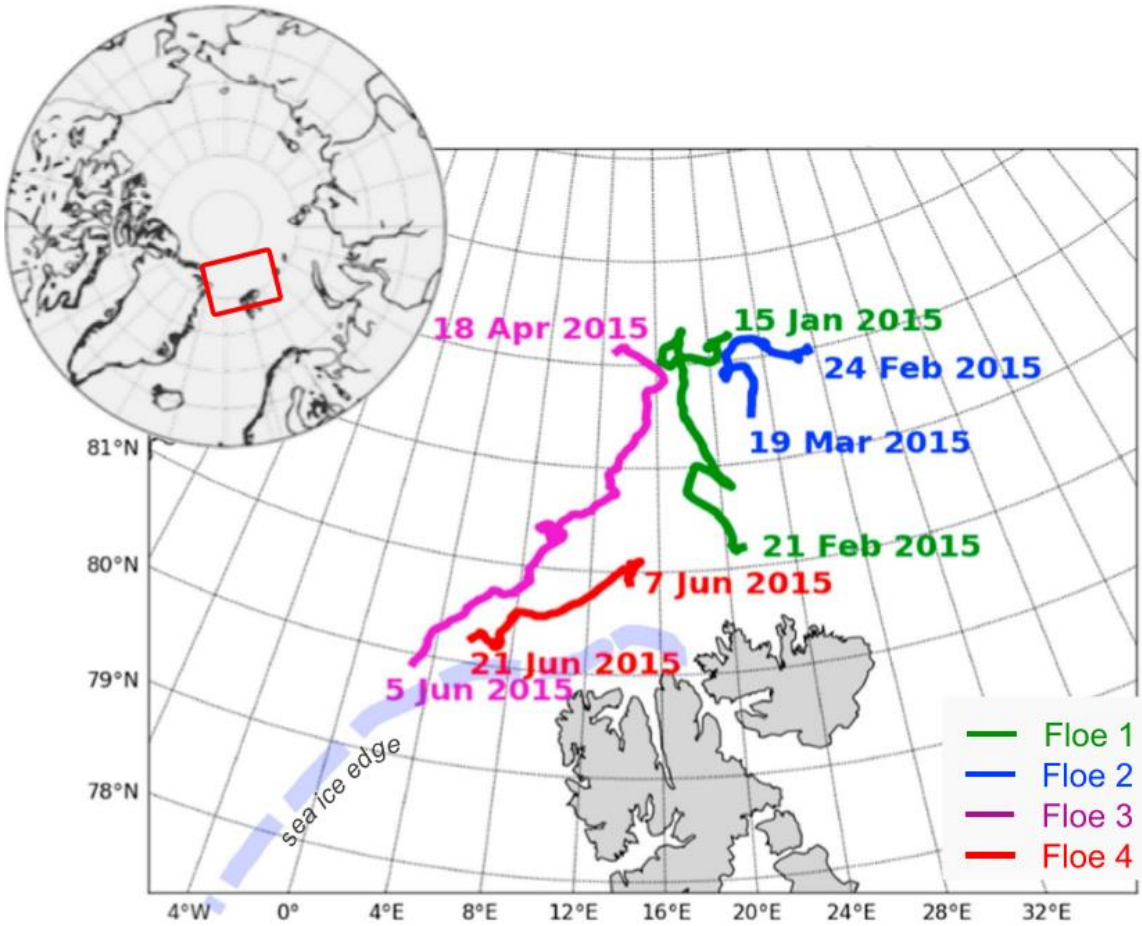

Figure 5: Location and start and end dates of N-ICE2015 drifts [Cohen et al., 2017]

3.2 Atmospheric Reanalyses

Exploitation of meteorological data that were collected for the First GARP Global Experiment (FGGE) in 1979 are the origin of reanalysis [*Dee et al., 2011*]. These observations were reanalysed s number of times. At first mainly to improve the knowledge on how to use the observations to initialise numerical weather forecast models. Reanalysis is a relatively young field and is of great value for atmospheric research. This is because the reanalysis data provide coherent record of global atmospheric circulation, which is a multivariant and spatially complex process. Furthermore, the reanalyses have proven to be important for climate studies.

There exist many generations of atmospheric reanalyses produced by various institutes, from improvement of models, input data and assimilation methods. A few of the global reanalyses that exist today are [*Lindsay et al., 2014*]:

- The NCEP-NCAR Reanalysis 1 project 1 [*Kalnay et al., 1996*] (NCEP-R1), from National Centers for Environmental Prediction- National Center for Atmospheric Research (NCEP-NCAR).
- The Japanese 25-yr Reanalysis (JRA-25) is the first long-term reanalysis that was made by Japanese Meteorological Agency (JMA) [*Onogi et al., 2007*].
- The Modern-Era Retrospective Analysis for Research and Application (MERRA) comes from National Aeronautics and Space Administrations (NASA).
- The ERA-40 reanalysis is an older reanalysis produced by European Centre for Medium-Range Weather Forecasts (ECMWF) [*Uppala et al 2005*].

In this study, reanalyses and forecast data set from ERA-Interim (ERA-I) [*Dee et al.*, 2011] and its successor ERA5 that comes from ECMWF will be evaluated. In addition, the ERA-40 reanalysis will be presented, as an introduction to how the atmospheric reanalyses works.

3.2.1 Observations in the reanalyses

Most of the current studies of the Arctic climate relies on global atmospheric reanalyses. However, in the Arctic region global climate models have been shown to struggle with simulating the current conditions [*Chapman and Walsh et al., 2007; Walsh et al., 2002; Karlsson and Svensson et al., 2011*]. This is a consequence from the lack of observations in the Arctic. The reanalyses rely on accessibility of observations with high spatial and time resolution, which the Arctic region lacks. Due to the shortage of observations in the Arctic the reanalyses have shown inaccuracy, mostly as a result of the following problems [*Wesslén et al., 2014*]:

i) Problem to constrain the models due to few available data
ii) Few available data for evaluating the reanalyses. Most of the data have been used in the assimilation in the reanalyses.
iii) The underlying global models can not efficient simulate processes unique to the Arctic environment due to the parameterization contained in the models.

Furthermore, the accuracy of an underlying atmospheric model will also influence the reanalyses. The reason for this is that generally the atmospheric models have a spatial resolution which is too coarse for studying several aspects of the climate system. In addition, the global reanalyses have errors on the description of physical processes. These are for example descriptions of boundary layer, sea ice, clouds and other sub-grid-scale processes. Moreover, the global reanalyses differ in technical aspects, such as the description of data assimilation techniques.

The measurements from Arctic expeditions are important for the different reanalysis products. This is because during the period when the expedition takes place, the reanalysis can be closer to actual value for the different variables. However, this only happens if the measurement that is taken during the expedition is sent as input, to be assimilated into the reanalysis. This is only possible during the expedition, which means that at some time after the expedition has finished, the reanalysis will go back to mainly using input from a weather forecast model and

satellite data. Thereby these observations from the expeditions will improve the forecast model and the assimilation process for the reanalysis for a short period.

In view of the fact that there are so few observations in the Arctic, it is important to find out how the atmospheric reanalyses represent the Arctic climate. Hence find the biases for the different meteorological and radiation variables for the different seasons of the year. For instance, how are the clouds and sea-ice represented in the reanalysis? Many studies have been conducted to see how good the different global reanalysis perform [*Wesslén et al., 2014; Lindsey et al., 2014; Jakobson et al., 2012; Simmons et al., 2015; Tjernström and Graversen et al., 2009; Walsh and Chapman et al., 1998*]. In addition, many studies have been dedicated to find out how well different forecast models perform [*Bromwich et al., 2015; Cassano et al., 2011; Sotiropoulou et al., 2015; Wilson et al., 2011; Wyser et al., 2008*]. Furthermore, few of the studies evaluate the reanalyses in the Arctic during the winter season. Although, most of these studies have used data of observations that have been assimilated into the reanalyses, such as observations from one-year expedition SHEBA. On the hand, a few independent data set of measurements from expeditions exist (not assimilated into the reanalyses), such as the observations taken during the TARA and ASCOS field campaigns.

For evaluating the reanalysis with observations, is it normal to calculate mean biases, root-mean square errors and correlation coefficients for the different variables (e.g. temperature, pressure, wind speed, humidity) in the two datasets. For example, previous evaluation with use of ASCOS and TARA observations have concluded that the ERA-Interim reanalysis produces a positive bias for the near surface temperature [*Wesslén et al., 2014; Lindsey et al., 2014; Jakobson et al., 2012*]. Accordingly, this will affect other studies that have used the temperature produced by ERA-Interim as well. Appropriately they will keep in mind the existence of a positive bias in ERA-Interim, when they make a conclusion for their study.

3.2.2 Satellite

Regarding the reanalysis products, observations from satellites have been useful for learning about numerical weather prediction from the assimilated cloud- and rain-affected satellite radiation [*Dee et al., 2011*]. Especially for the ERA-Interim reanalysis when being developed attempted to correct several of the assimilation problems regarding satellite observation in the ERA-40 reanalysis.

The satellite observations over the Arctic region are important for the reanalysis products. This comes from that for most areas in the Arctic there exist quite few other observations, not in fact provided by satellites. Further the satellite data will help produce reanalysis data that represents the Arctic climate better, instead of reanalysis values that are mostly represented by a weather forecast model.

3.3 ERA-40

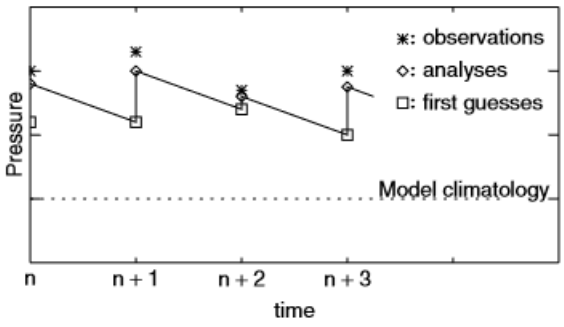

Figure 6: A schematic illustration of the assimilation process for 3D-var system in ERA40. Stars, diamonds and squares indicate observations, reanalysis, and forecast model first guesses, respectively. Image found in [Graversen et al., 2007].

First, we need a little insight on how the ERA-40 reanalysis works. In the beginning the ERA-40 will start with a forecast model for any variable. This forecast model is called the first guess model. The first guess model together with observations sent in from different weather stations will go through a weighting process. A short remark, all observations credibility of their own, depending on how the observation is obtained e.g. thermometer, satellite, radiosondes and other measuring methods. The weighing process will affect the credibility for the observation depending on when and where the observation was measured regarding to the grid points and assimilation interval in the reanalysis. If the observations are found less trustworthy, then more weight will be added for first guess model. Thus, the reanalysis value will be closer to the first guess model. On the other hand, the reanalysis will be closer to the observations if the

observations are found trustworthy in the weighting process, which is illustrated in Figure 6. The finished product from the weighting process will be the reanalysis data for the atmosphere with a 6-hourly interval. Hence the reanalysis data will be a value somewhere in between the observed data and the first guess model. This procedure is described as a three-dimensional variational data assimilation (3D-Var) [*Uppala et al., 2005*].

Exactly what the reanalysis value will be, depends on what type of measurement that is sent in. Each measurement has its own distribution and uncertainty, to put it simple; how much do we trust the measurements that were taken? For example, if we assume that a measurement for a particular variable is the correct representation. Then the assimilated reanalysis data will be closer to the measurement than the first guess model.

On the other hand, if the measurement has a lot of uncertainty with how it is collected, the accuracy of the assimilated reanalysis data could decrease compared to the first guess model.

In addition, the distance between both in time and space for the observation and the grid point where reanalysis value is obtained from, will also have a role to play for the uncertainty that the observation has.

The next value in a reanalysis is established in the following way: a new forecast will be produced by the model from the previous reanalysis value, and will run for 6 hours until new reanalysis data are assimilated from this first guess model and the inserted observations during the period from the last value.

3.4 ERA-Interim

Era-Interim is a modified atmospheric reanalysis model that the European Centre for Medium-Range Weather Forecasts (ECMWF) developed to replace the ERA-40 [*Dee et al., 2011*].

The Era-Interim data are continuously updated to near real time and contains data from 1979 and onwards. The entire model has a 12-hour assimilation window. ERA-Interim has a spatial

resolution for approximately 79 km in the horizontal plane, and 60 vertical levels from 0.1 hPa down to the surface. From http://www.ecmwf.int/research/era various climate indicators derived from ERA-Interim date near present time and historical available data can be found.

ERA-Interim uses a four-dimensional variational data assimilation (4D-Var). An improvement compared to ERA-40 is that, ERA-Interim consider that the observed data not necessary has been collected exactly when the assimilation occurs. The assimilation is performed continuously within the 12-hour assimilation window. This is done in an iterative process where assimilation is applied both backward and forward in time, in several steps within the assimilation window using an adjoint linear model.

Benefits of the 4D-Var is that just by using observation of surface pressure, the 4D-var is able to produce accurate analyses of the large-scale tropospheric circulation compared to previous reanalysis, such as ERA-40 [*Dee et al., 2011*]. The assimilation system can use the physical information implicit in the model equation quite well, and it is and enormous help for where there are few observations.

3.5 ERA5

Era5 is the latest reanalysis from ECMWF, and will in a few years replace the ERA-Interim reanalysis. More accurate is ERA5 the fifth generation of atmospheric reanalysis of the global climate that ECMWF has produced. ERA5 has a horizontal spatial resolution at 31 km, and has 137 vertical levels from the surface up to a height of 80 km or 0.01 hPa. In addition, will ERA5 data that cover the period from 1950 to present time be available to use by early 2019 [*ERA5*, www.ecmwf.int].

4 Results and Discussion

4.1 Evaluation of ERA5 and ERA-I with the N-ICE2015 data set

The focus of this section is to find out how the two reanalyses ERA-Interim and ERA5 present the measurements taken during the N-ICE2015 expedition. Hence, the ERA-Interim and ERA5 reanalysis will be compared against the observed valued from the N-ICE2015 expedition. The N-ICE2015 data that were assimilated into the reanalyses are the temperature, pressure and water vapour from the radiosondes. On the other hand, other data such as the longwave radiative fluxes, wind speed and cloud water path, were not assimilated into the reanalyses [*Graham et al., 2017*]. The variables that have been compared in this section are the temperature, mean sea level pressure, water vapor path, wind speed, upward- /downward longwave radiation and upward- /downward shortwave radiation.

4.1.1 Winter period

The winter period for the N-ICE2015 expedition is defined to be from the start of the expedition January to the end of March. Figure 7 give an overview of the winter period timeseries of the meteorological variables 2m temperature (T2m), mean sea level pressure (MSLP), vertically integrated water vapour (QVI) and 10 m wind speed (U10M). Further seen in Table 1 are all the calculated biases, Root Mean Square Errors (RMSE), and correlations for the mentioned variables in addition to all the radiation components. In Figure 8 are the winter period timeseries for the downward longwave radiation (LWD), upward longwave radiation (LWU), downward shortwave radiation (SWD) and upward shortwave radiation (SWU). At last the net longwave radiation (LWN) and net shortwave radiation (SWN) timeseries are given in Figure 9.

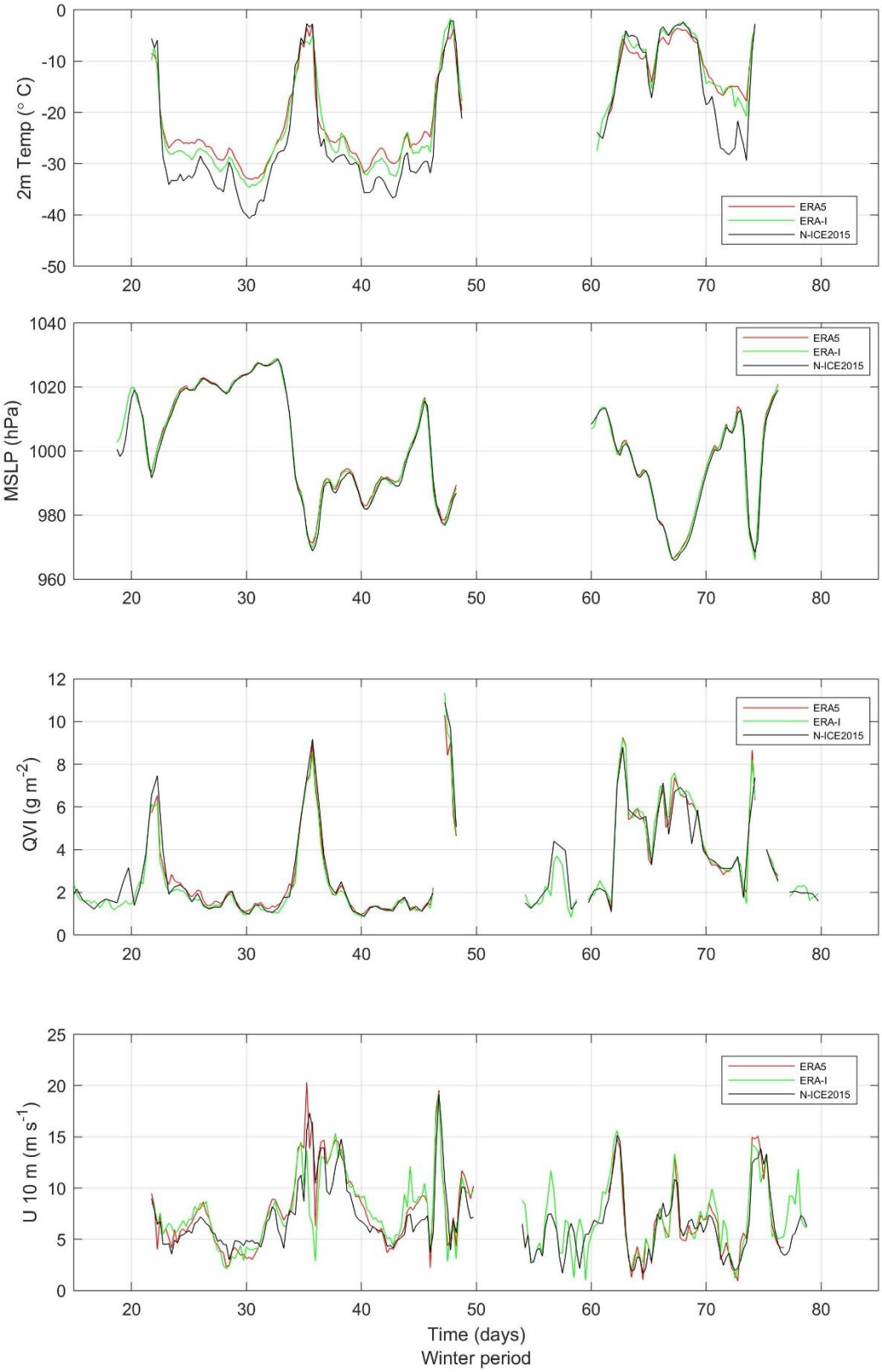

Figure 7: Timeseries of winter period (January - March). Comparing N-ICE2015 (black) with ERA5 (red) and ERA-I (green) reanalyses. From top to bottom: 2m temperature, mean sea level pressure, vertically integrated water vapor and wind speed.

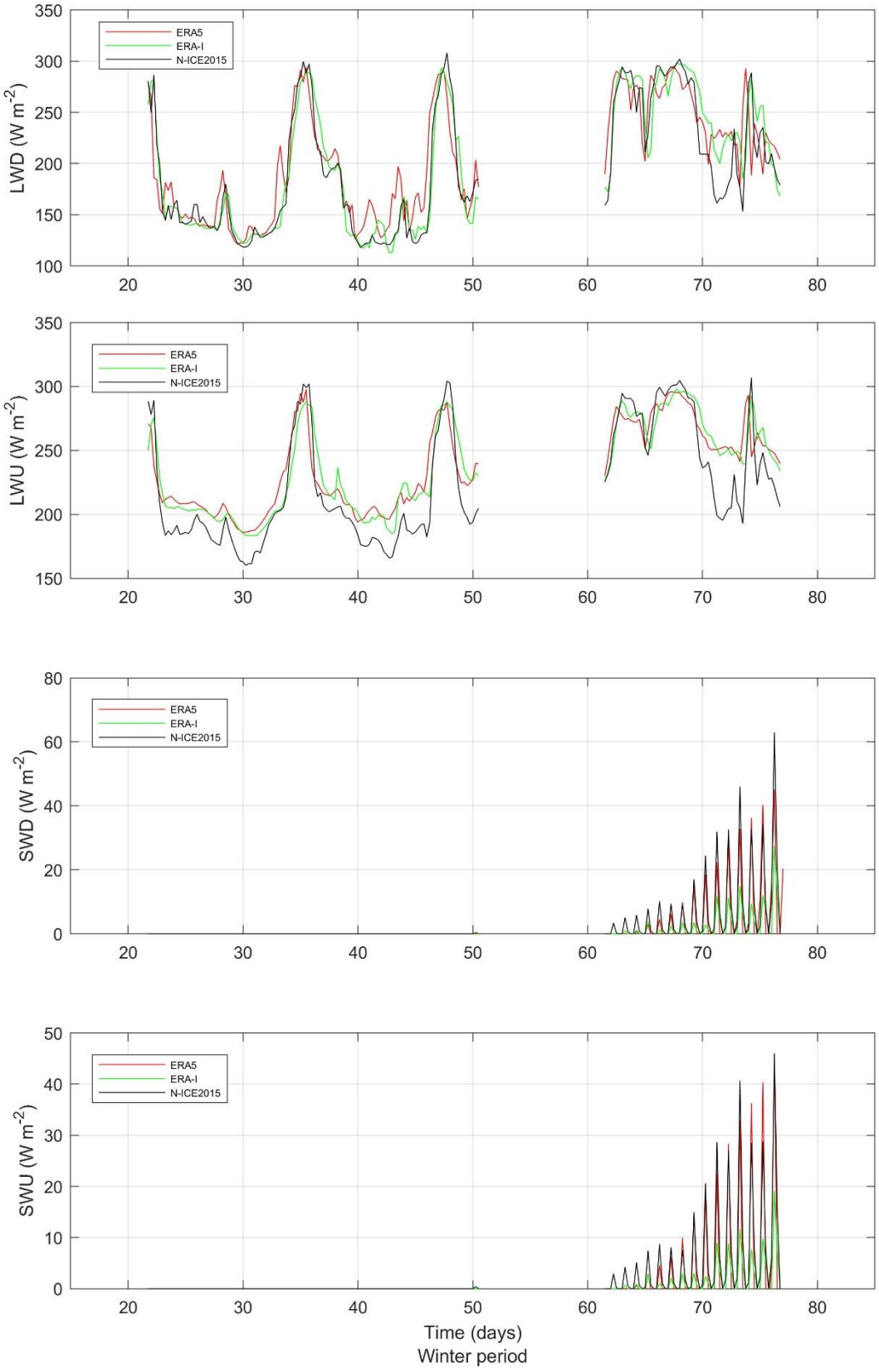

Figure 8: Timeseries of winter period (January - March). Comparing N-ICE2015 (black) with ERA5 (red) and ERA-I (green) reanalyses. From top to bottom: downward longwave radiation, upward longwave radiation, downward shortwave radiation and upward shortwave radiation.

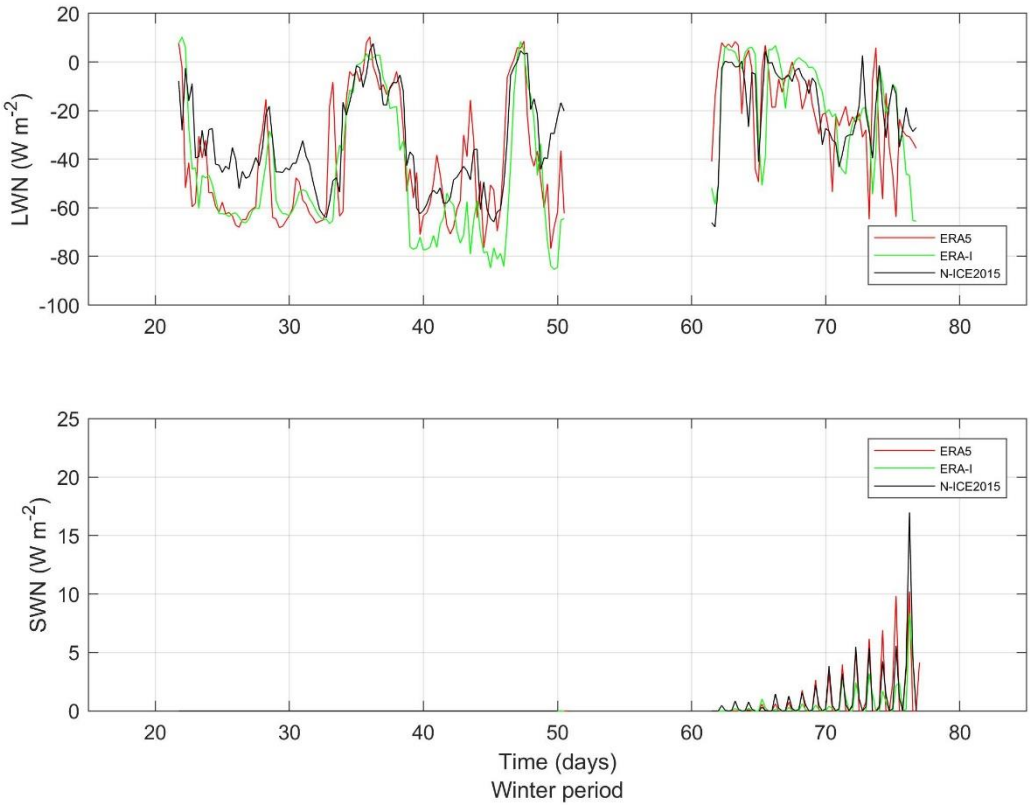

Figure 9: Timeseries of winter period (January - March). Comparing N-ICE2015 (black) with ERA5 (red) and ERA-I (green) reanalyses. From top to bottom: net longwave radiation and net shortwave radiation.

The two reanalyses ERA5 and ERA-Interim are not capable of presenting the exact values for most of the meteorological and radiative variables, but may overall represent the meteorological and radiative variables quite well. Consider firstly the 2m temperature (T2m), seen from Figure 7 when the T2m becomes less than -20 ℃ (T2m < -20 ℃) both reanalyses overestimate the real temperature state [*Graham et al., 2017*]. This is consistent with the positive bias from Table 1 for both reanalyses. The positive bias that ERA-Interim produces have been found in other studies [*Wesslén et al., 2014; Jakobsen et al., 2012; Lindsey et al., 2014: Bromwich et al., 2015*] and remain still in the successor ERA5. The ERA-Interim has a positive bias of 2.81 ℃ and ERA5 has a bias that is +0.5 larger at 3.33 ℃. Further seen in Figure 7, when the T2m N-ICE2015 observations are larger than -20 ℃ (T2m > -20 ℃) the ERA5 reanalysis seem to overestimate the real temperature state more than the ERA-Interim reanalysis. Furthermore, Figure 10 a) show that ERA5 has mostly higher temperatures differences than the differences found for ERA-Interim, which are consistent with the T2m biases.

Currently the older reanalysis ERA-Interim represents the real state best for the 2m temperature. Next, the correlation coefficient and RMSE will be used for evaluating the quality of the two reanalysis products. Both reanalyses have high correlation coefficient (r), there ERA-Interim is best correlated with r=0.97, and ERA5 is not far behind with r=0.93. Hence both reanalyses have a strong positive relationship with the T2m N-ICE2015 data set, which means that if a positive increase in the observation occurs there will most likely be a positive increase with a fixed proportion for the both reanalyses. Of the two reanalyses ERA5 has the largest Root Mean Square Error value at RMSE= 5.91 ℃, while ERA-Interim has a slightly smaller value at RMSE= 4.12 ℃. This is expected, since the RMSE values are connected to the correlation coefficients. The RMSE value will increase, when the correlation coefficient is decreasing from 1. This implies that if the correlation coefficient is exactly one (r=1), the Root Mean Square Error will be equal to zero (RMSE=0).

Considering the mean sea level pressure, as seen in Figure 7 both ERA5 and ERA-Interim represent the true state remarkably well [*Wesslén et al., 2014*]. This is likely a result from that the mean sea level pressure is assimilated from the radiosondes. There exist some slightly larger differences between the ERA-Interim reanalysis and N-ICE2015 data when the observations are first collected, which are seen at the times around 20 and 60 days. The cause of these differences at the start of each periods may be that the first MSLP observations were not sent in for assimilation in the reanalysis products. While the ERA5 is not represented during these period, because of the interpolation scheme used to get the reanalysis data. In Figure 10 b), show that the ERA5 differences are almost all positive. Found from the probability density function (Figure 10 b)) that ERA-Interim differences graph has a peak near 0.5 Pa, and that most difference are between 0 Pa – 2 Pa for both reanalyses. In addition, ERA5 has a higher bias at 0.77 Pa, while ERA-Interim is slightly less at 0.55 Pa (highest peak). Both reanalyses have a significantly high correlation coefficient r=0.99, similarly found in [*Bromwich et al., 2015*], and this is further represented in Figure 7.

Regarding the water vapor path (QVI), then both reanalyses represent the real state remarkably well during both the colder and warmer periods as seen in Figure 7. This is probably due to the fact that the water vapour is assimilated from the radiosondes. Both ERA5 and ERA-Interim have a negative bias, similarly found in [*Wesslén et al., 2014*]. In this study ERA5 has the best at -0.02 $g\ m^{-2}$ while ERA-Interim has -0.11 $g\ m^{-2}$. In addition, ERA5 has the highest correlation coefficient r=0.99 comparing to the correlation coefficient

for ERA-Interim (r=0.97). Figure 10 c) show that ERA5 has the highest peak near zero and more of the graph is on the positive side, than for ERA-Interim reanalysis.

Both ERA5 and ERA-Interim have a positive bias for the total wind speed (U10M), this can also be seen in [*Jakobsen et al., 2012; Bromwich et al., 2015*]. This study found that the positive bias for ERA5 is 0.56 $m\ s^{-1}$ and ERA-Interim has a slightly larger bias at 0.60 $m\ s^{-1}$. Hence, both reanalyses overestimate the total wind speed. This can be slightly difficult to see from Figure 7 for the whole winter period. From Figure 10 d), most differences in wind speed between the two reanalyses and observations are centred around -2 $m\ s^{-1}$ ~ 2 $m\ s^{-1}$. ERA5 does present the 10-meter wind speed best of the two reanalyses. Moreover, ERA5 has the best results from the calculated variables in Table 1. On the other hand, the correlation coefficient for the two reanalyses are smaller for the wind speed variable, than for most of the other variables in Table 1. ERA5 has the highest correlation coefficient r=0.83, while ERA-Interim has a smaller correlation coefficient r=0.79.

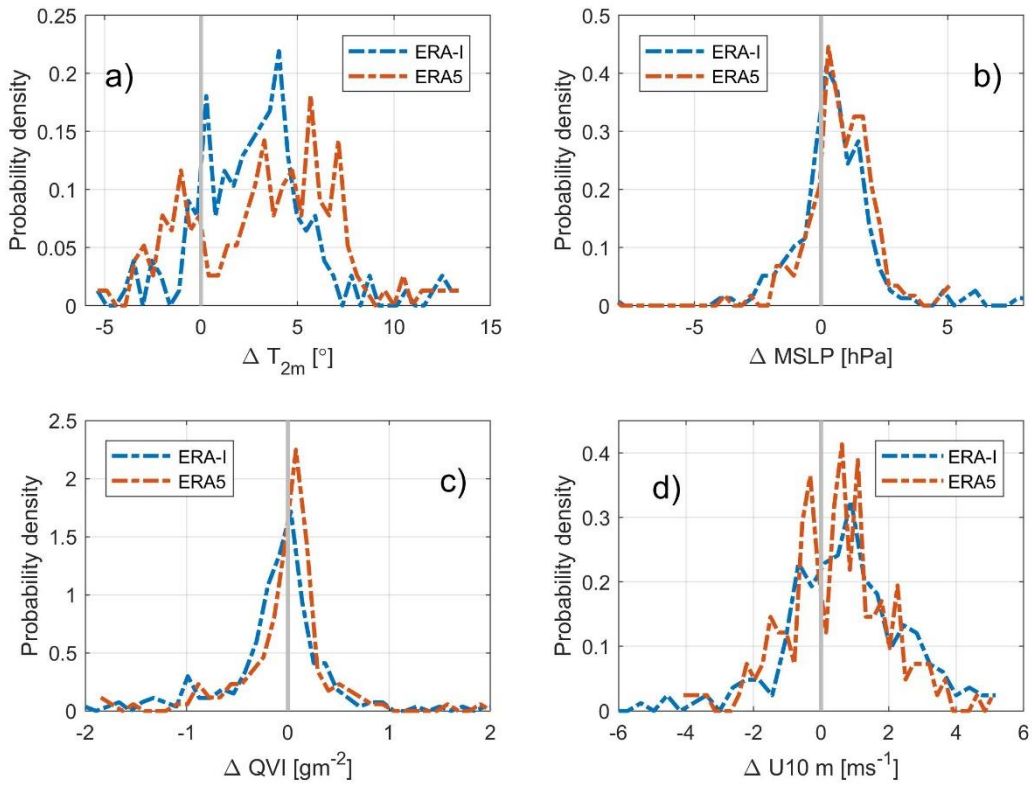

Figure 10: Probability density functions (PDF) of the difference between the two reanalyses and N-ICE2015 observations for the winter period. (a) 2m temperature in ℃, (b) mean sea level pressure in Pa, (c) vertically integrated water vapor $g\ m^{-2}$, and (d) total wind speed in $m\ s^{-1}$.

Regarding the downward longwave radiation (LWD), both reanalyses have positive bias [*Lindsey et al., 2014*], where ERA5 has the highest at 8.19 $W\ m^{-2}$ compared to ERA-Interim with 3.95 $W\ m^{-2}$. Figure 8 show that the ERA5 reanalysis overestimates the real state more than ERA-Interim does, especially during the colder periods. Similarly, seen for the 2m temperature variable. All in all, both reanalyses have a very high correlation coefficient (r), where ERA-Interim is r=0.95 and ERA5 is r=0.93. ERA-Interim present best for the LWD variable. This is also seen in Figure 11 a) that the difference in LWD between ERA-Interim and observations are centred around 0 $W\ m^{-2}$ from -10 $W\ m^{-2}$ to 10 $W\ m^{-2}$, while the ERA5 differences are more dispersed. Both reanalyses have a peak close to zero, which is likely due to the cloudless condition [*Wesslén et al., 2014*]. The downward longwave radiation is the radiation that the clouds and atmosphere emits down to Earth. Hence, a cloudy atmosphere will emit more longwave radiation (LW) than a cloudless atmosphere. Refer to Figure 8 when the LWD (< 200 $W\ m^{-2}$) occurs during the cold periods when 2m temperature is below -20 ℃. Accordingly, the sky is cloudless when the lowest temperatures occurs [*Walsh and Chapman et al., 1998*].

The upward longwave radiation (LWU) for both reanalyses are calculated by subtracting the downward longwave radiation (LWD) from the net longwave radiation (LWN). The LWU time series for the winter period is given in Figure 8 and is quite similar to the time series for the 2m temperature from Figure 7, because the LWU is amplified by the warmer surface temperature due to Stefan-Boltzmann's law [*Graham et al., 2017*]. As seen in Figure 8 both reanalyses overestimate the LWU during the cold periods due to the overestimation of the near surface temperature, which is consistent with the positive bias from Table 1. Further proof that both reanalyses overestimate the true state comes from Figure 11 b), where the probability density is higher when the reanalyses have higher values than the observations. Thus, the area under both curves in Figure 11 b) are larger on the positive side of 0 $W\ m^{-2}$, when the reanalyses will have a larger value then the N-CE2015 observations.

On the other hand, the net longwave radiation (LWN) has a negative bias for both ERA5 and ERA-Interim [*Sotiropoulou et al., 2015*]. Hence, both reanalyses underestimate LWN as can been seen in Figure 9, especially during the cold periods when 2m temperatures are below -20 ℃. Thus, both reanalyses lose too much heat during cool periods, because of positive bias for the near surface temperature. The underestimation of LWN is due to the overestimation from

the LWU [*Graham et al.,* 2017]. In addition, it looks like the ERA5 reanalysis is closer to the real state, which is consistent with the bias since ERA5 has a smaller bias -5.4 Wm^{-2} than the bias for ERA-Interim at -9.2 Wm^{-2}. In fact, that ERA5 is better at presenting the LWN is quite surprising, because previously seen that ERA-Interim was better at presenting the near surface temperature. However, that ERA5 is better for LWN is due to the compensating bias in LWD.

The winter period occurs during polar night. This is because the transition between polar night and day occurred during the campaign break in April [*Kayser et al. 2017*]. Thereby, there exist no shortwave radiation (SW) till after day 60 as seen in Figure 8. With so few observations during the winter period is it not suitable to make a conclusion on the performance for SW from ERA5 and ERA-Interim, but evaluation will still take place for both SW components. Both reanalyses have negative biases for the two components for SW. The two reanalyses underestimate the downward shortwave radiation (SWD) and upward shortwave radiation (SWU) seen in Figure 8 for the timeseries. Unexpectedly seen in Figure 11 c), ERA-Interim does not ever overestimate the SWD during the winter period, and to a certain extent has a more negative bias than the ERA5 reanalysis has.

The upward shortwave radiation (SWU) is calculated in the same way as LWU, by subtracting net SW with downward SW. ERA5 has the smallest bias at -0.59 $W\ m^{-2}$and abnormal small correlation coefficient r=0.01, while ERA-Interim has a bias of -1.39 $W\ m^{-2}$and quite good correlation coefficient at r=0.96. Same as for SWD, ERA-Interim does not ever overestimate the SWU (Figure 11 d)). In addition, the probability density plot is a little misleading for the SWU and SWD because they have quite a high peak near zero, which is a cause from zero solar radiation during night hours when the sun is below the horizon.

Regarding the bias for the SWN, for both reanalyses this is very small. Moreover, the RMSE values are also quite small. On the other hand, ERA-Interim has a quite high correlation coefficient r=0.91, while the correlation coefficient for ERA5 is significantly smaller at 0.06. The timeseries to SWN (Figure 9), show that both reanalyses represent the observations quite well.

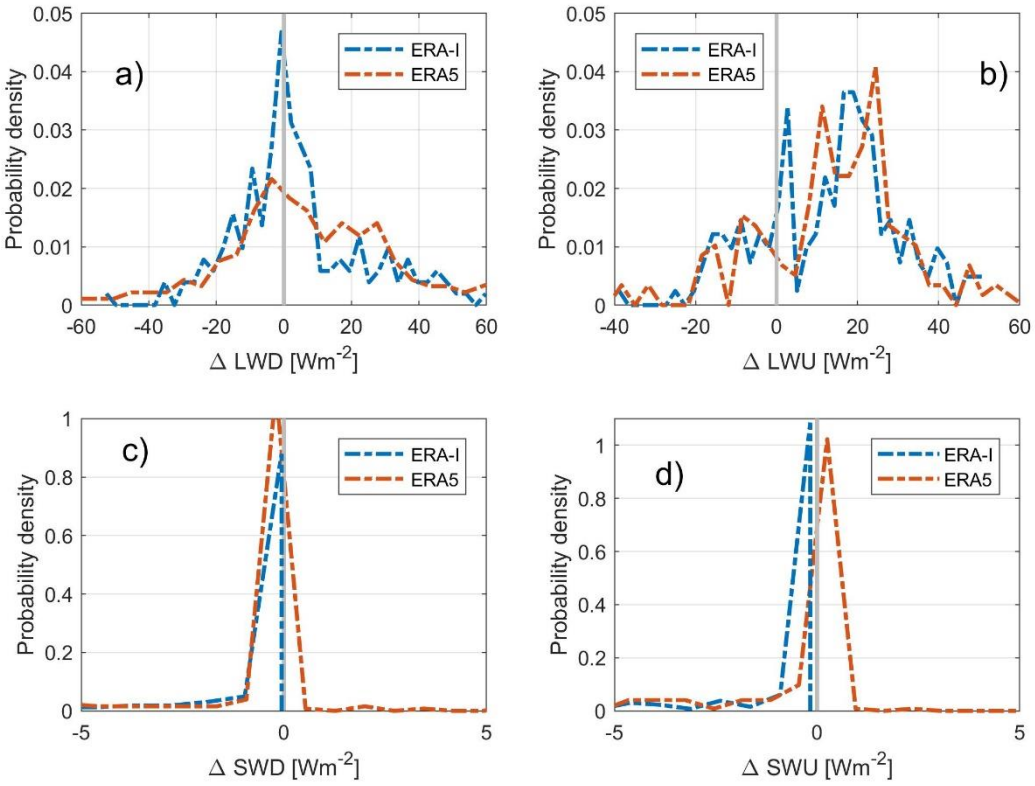

Figure 11: Probability density function of the difference between the two reanalyses and N-ICE2015 observations for winter period. (a) downward longwave radiation in $W\ m^{-2}$, (b) upward longwave radiation in $W\ m^{-2}$, (c) downward shortwave radiation in $W\ m^{-2}$, and (d) upward shortwave in $W\ m^{-2}$

***Table 1**: Summary of model errors: mean bias, correlation coefficient and root-mean-square error (RMSE) between ERA-Interim/ERA5 and N-ICE2015 observations for the winter period (January – March). For the variables from Figure 7-8*

Winter period				
Variable	**Model**	**Bias**	**Corr.**	**RMSE**
T2M (℃)	ERA-I	2.81	0.9730	4.12
	ERA5	3.33	0.9675	5.01
MSLP (Pa)	ERA-I	0.56	0.9945	1.86
	ERA5	0.77	0.9966	1.63
Wind -U10M ($m\ s^{-1}$)	ERA-I	0.60	0.7962	2.18
	ERA5	0.46	0.9155	1.60
QVI ($g\ m^{-2}$)	ERA-I	-0.11	0.9661	0.56
	ERA5	-0.02	0.9945	1.86
LWD ($W\ m^{-2}$)	ERA-I	3.95	0.9505	19.53
	ERA5	8.19	0.8777	30.19
LWU ($W\ m^{-2}$)	ERA-I	13.14	0.9322	21.50
	ERA5	13.78	0.9095	24.01
LWN ($W\ m^{-2}$)	ERA-I	-9.19	0.8320	18.80
	ERA5	-5.59	0.6855	19.34
SWD ($W\ m^{-2}$)	ERA-I	-1.58	0.9536	5.44
	ERA5	-0.63	0.0017	10.58
SWU ($W\ m^{-2}$)	ERA-I	-1.39	0.9587	4.69
	ERA5	-0.59	0.0117	8.63
SWN ($W\ m^{-2}$)	ERA-I	-0.19	0.9184	0.91
	ERA5	-0.04	0.0600	2.07

4.1.2 Spring period

The spring period of the N-ICE2015 expedition is defined to be from April 1st to the end of the expedition in late June in 2015. For the spring period the timeseries of the meteorological variables 2m temperature (T2m), mean sea level pressure (MSLP), vertically integrated water vapour (QVI) and 10 m wind speed (U10M) are given in Figure 12. Further, the spring period timeseries for the downward longwave radiation (LWD), upward longwave radiation (LWU), downward shortwave radiation (SWD) and upward shortwave radiation (SWU) are given in Figure 13. Finally, the net longwave radiation (LWN) and net shortwave radiation (SWN) timeseries are given in Figure 14. All calculated bias, correlation coefficient (r), Root Mean Square Error for all variables given above are presented in Table 2.

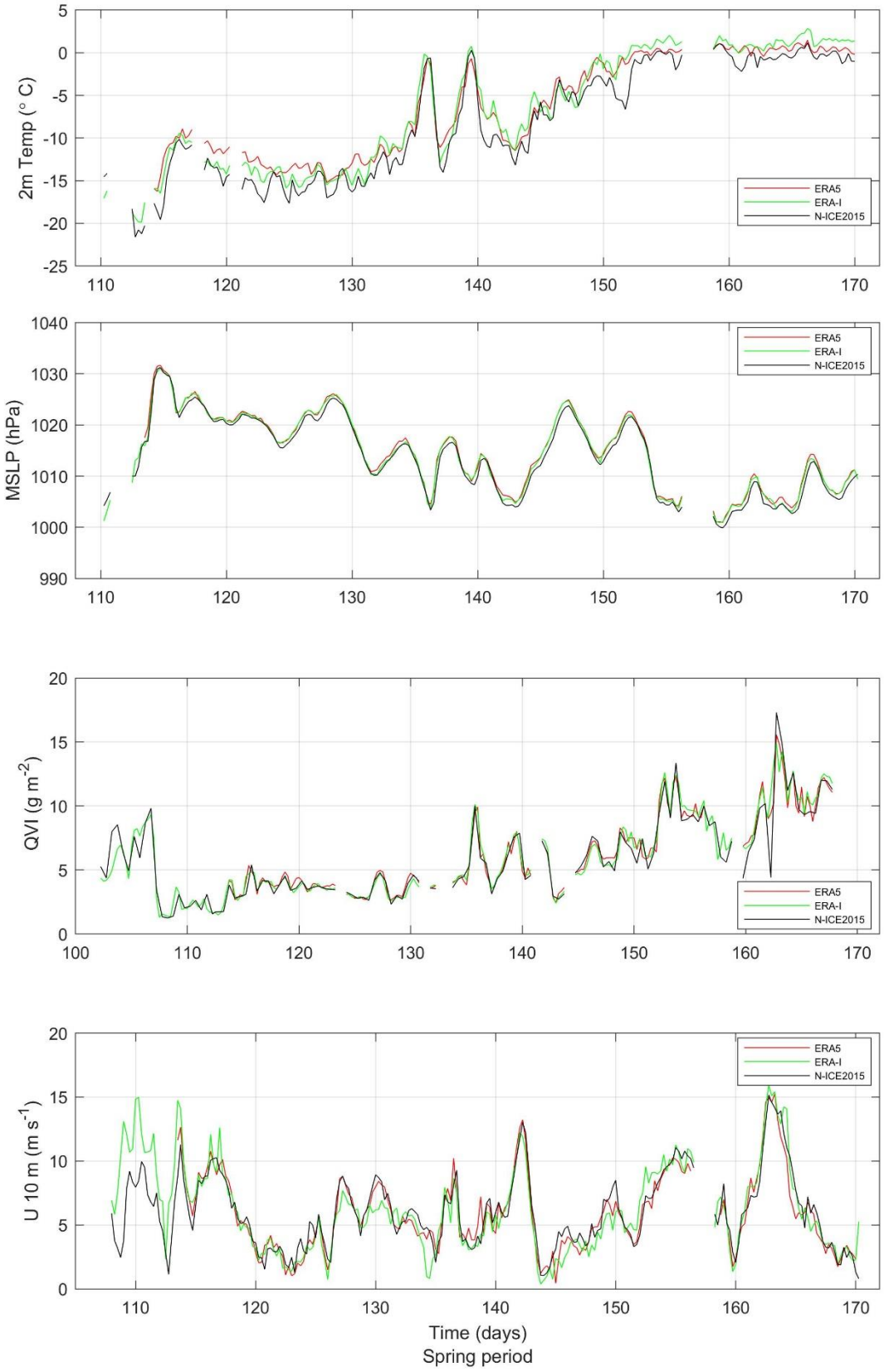

Figure 12: Timeseries of spring period (April - June). Comparing N-ICE2015 (black) with ERA5 (red) and ERA-I (green) reanalyses. From top to bottom: 2m temperature, mean sea level pressure, vertically integrated water vapor and wind speed.

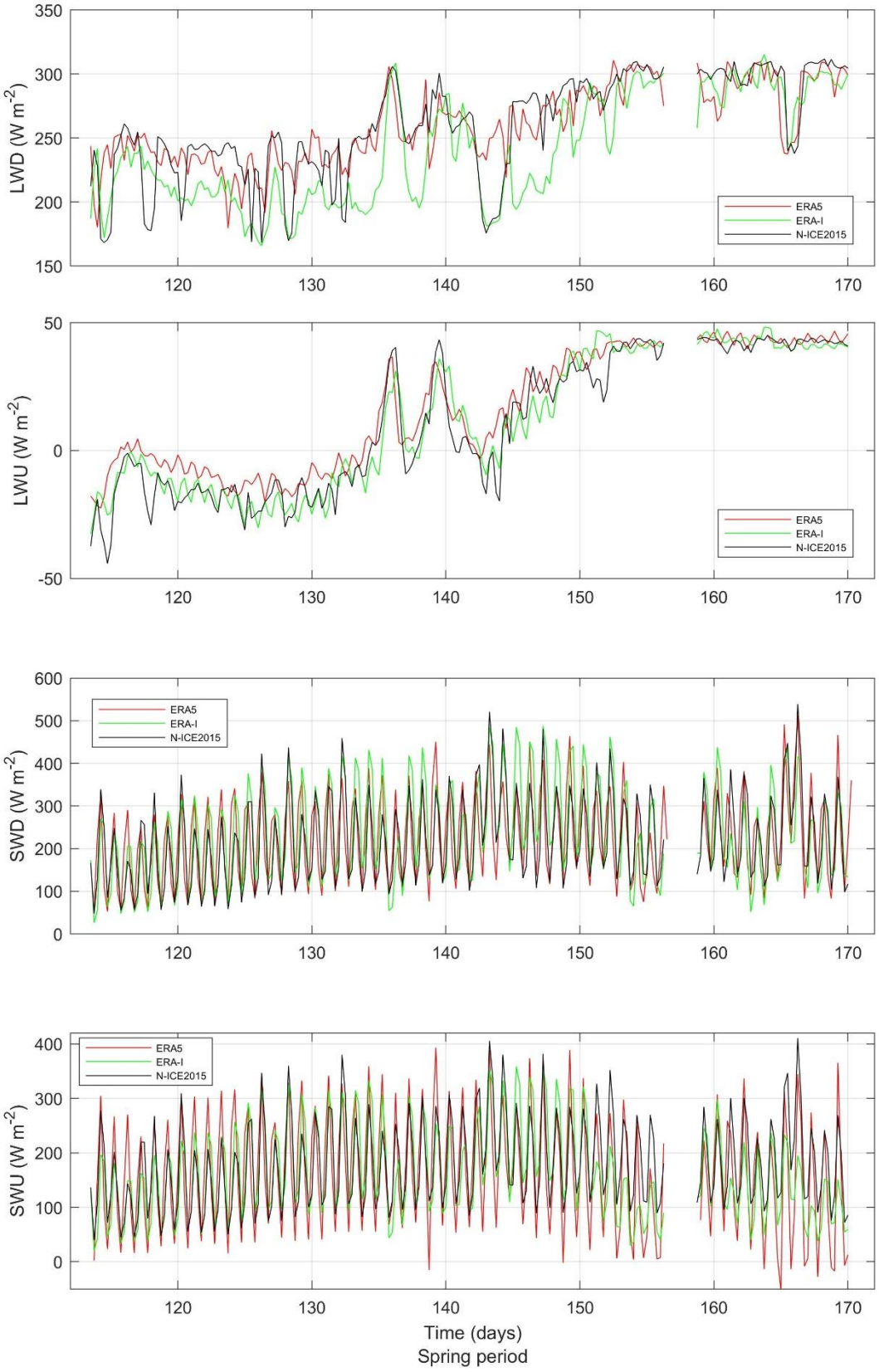

Figure 13: Timeseries of spring period (April - June). Comparing N-ICE2015 (black) with ERA5 (red) and ERA-I (green) reanalyses. From top to bottom: downward longwave radiation, upward longwave radiation, downward shortwave radiation and upward shortwave radiation.

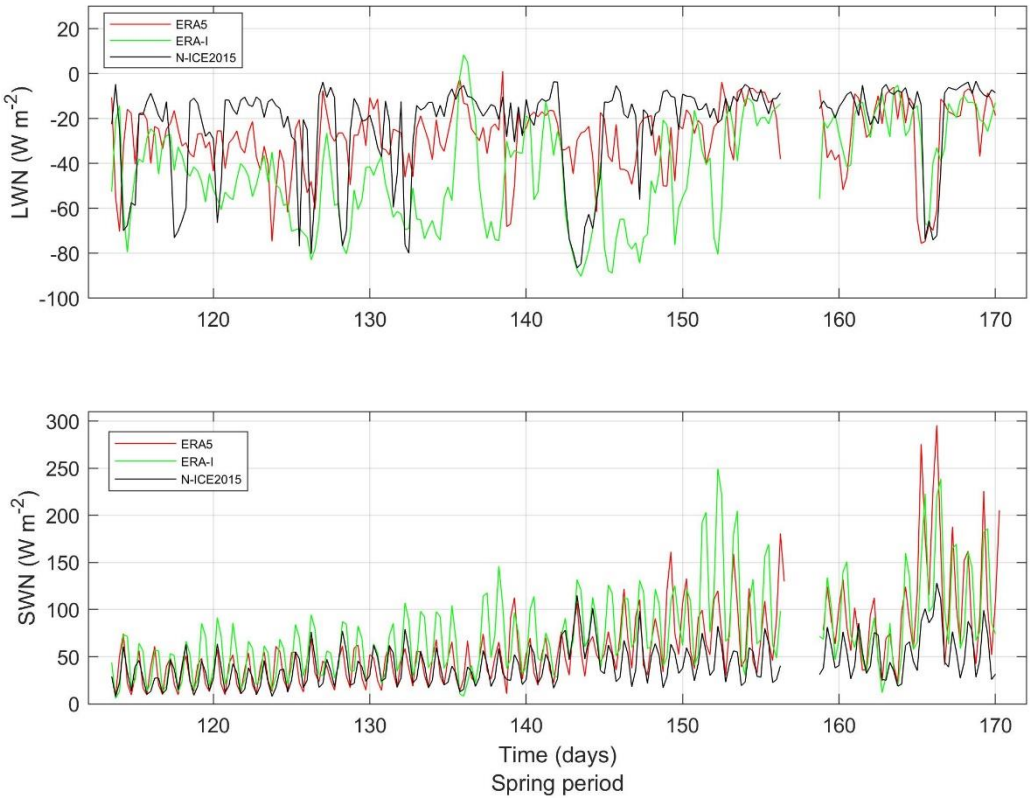

Figure 14: Timeseries of spring period (April - June). Comparing N-ICE2015 (black) with ERA5 (red) and ERA-I (green) reanalyses. From top to bottom: net longwave radiation and net shortwave radiation.

Regarding the 2m temperature, the bias for both reanalyses during spring period improved quite a lot from the bias for the winter period. ERA5 has a positive bias at 1.47 ℃, while ERA-Interim bias is a little better at 1.42 ℃. Hence, both reanalyses overestimate the real temperature state, but they still capture the general features of temperature trends [*Wesslén et al., 2014*]. Figure 12 show that both reanalyses are above the N-ICE2015 observations. In addition, ERA5 present the near surface temperature better when the temperature is above ~-5 ℃. Moreover, most differences between observations and reanalysis are centred around 0 ℃ - 3 ℃ seen from Figure 15 a). Thereby the reanalyses are somewhat closer to the real temperature state during the spring period, than for the winter period where the differences were more scattered for higher and lower temperature values. In addition, the correlation coefficient and the RMSE-values given in Table 2 for both ERA5 and ERA-Interim have improved from the winter period, which is contradictory to what is presented in [*Lindsey et al., 2014*], where the correlation coefficient worsen when summer time approach. The

correlation coefficients have increased by at least 0.01 for both ERA-Interim and ERA5, while the RMSE values have decreased by at least 2 ℃.

The calculated variables bias, correlation coefficient and RMSE have not changed much for both reanalyses during the spring period compared to the winter period for the MSLP. The reason for this is probably due to the fact that the radiosonde observations for MSLP are assimilated into the reanalyses. Both reanalyses still have a positive bias, which means that the models mostly overestimate the real pressure value. The overestimation can be seen in Figure 15 b), that most of the difference between the reanalysis and observations are between 0 Pa - 2 Pa. Figure 15 b) show that ERA-Interim has a long negative tail, which is probably from day 110 (Figure 7). Nevertheless, both reanalyses present the mean sea level pressure reasonably well for the spring period [*Wesslén et al., 2014*].

Next for the vertically integrated water vapor (QVI), the bias for both reanalyses have become positive, which are consistent that both reanalyses overestimate the true state. Equivalent Figure 15 c) show, that the area under curves are slightly larger on the positive side, than for the negative side. The ERA5 reanalysis has decreased its performance for estimating the water vapor for the spring compared to the winter period. The conclusion can be made from the calculated variables in Table 2 which have become worse for ERA5, but stayed relatively the same for ERA-Interim.

Regarding the total wind speed (U10M), the bias for ERA-Interim has become larger during the spring period at 0.18 $m\ s^{-1}$, while the bias for ERA5 is negative at -0.14 $m\ s^{-1}$. In addition, both correlation coefficients (r) for the reanalyses have become larger for the spring period relative to the corresponding winter period values, respectively ERA-Interim: r=0.84, ER5: r=0.94. Similar result is found in [*Lindsey et al., 2014*]. Most differences between the two reanalyses and observations are centred around -3 $m\ s^{-1}$ ~ 2 $m\ s^{-1}$ seen in Figure 15 b). Moreover, Figure 12 show that both reanalyses represent the wind speed quite well during both long cold (days 120-130) and warm (days 160-170) period, but also during periods of rapid temperature change (days 135-140). One exception is in the start of the spring period where the ERA-Interim values are much larger than N-ICE2015 observations. The reason for this may be that the N-ICE2015 observations were not assimilated into the reanalyses during this period. Overall it appears that the ERA5 reanalysis represents the true state best of the two reanalyses for this variable.

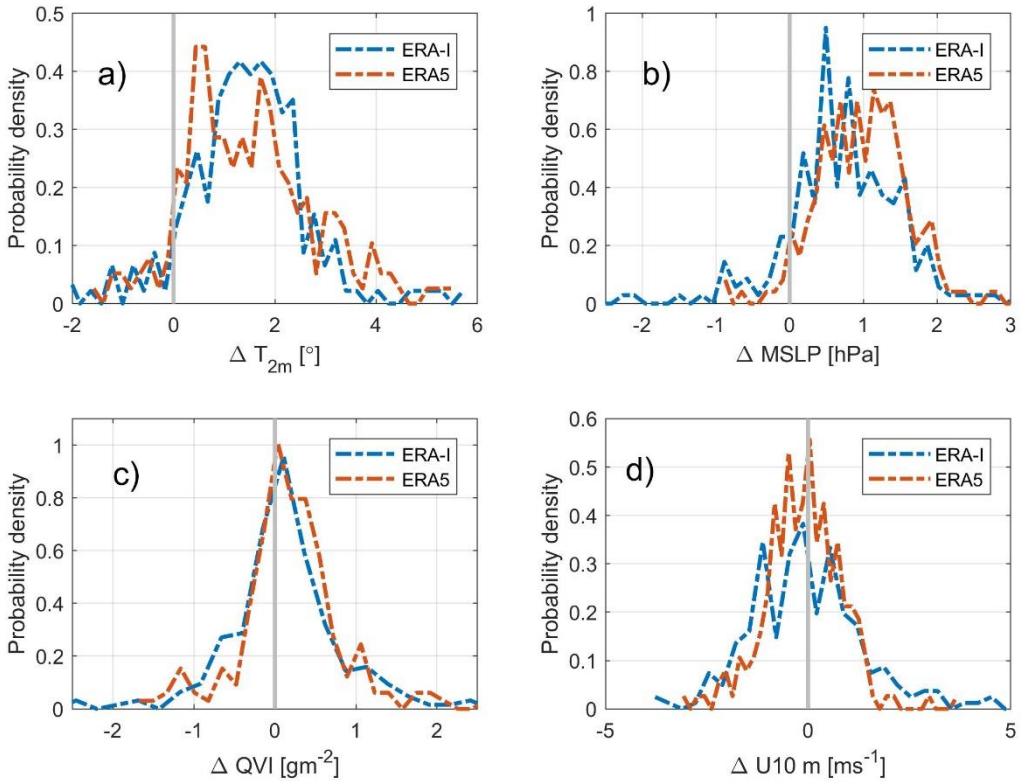

Figure 15: Probability density function (PDF) of the difference between the two reanalyses and N-ICE2015 observations for the spring period. (a) 2m temperature in ℃, (b) mean sea level pressure in Pa, (c) vertically integrated water vapor $g\ m^{-2}$, and (d) total wind speed in $m\ s^{-1}$.

For the downward longwave radiation (LWD), the ERA5 reanalysis has an astonishing low bias at 0.26 $W\ m^{-2}$. This is quite surprising since it looks like from Figure 13 that ERA5 mostly underestimate the LWD value except when the LWD value suddenly drops. Thus, affect the bias for ERA5 to be slightly positive. On the other hand, the bias for ERA-Interim is smaller for the spring than winter period at -19.53 $W\ m^{-2}$. This negative bias is also found in *Bromwich et al., 2015*, which is quite the different from bias for the winter period. Clearly, Figure 13 for the timeseries show that overall ERA-Interim underestimates the real LWD value. In addition, Figure 16 a) display that most differences between ERA-Interim and observations are on the negative side, which agree with the negative bias. On the other hand, the differences between ERA5 and observations do vary from -60 $W\ m^{-2}$ to 70 $W\ m^{-2}$, with a peak near 0 $W\ m^{-2}$. In addition, other peaks occur for both reanalyses, which is probably a contribution of the anomalous cloudless period [*Wesslén et al., 2014*]. Furthermore, the correlation coefficient for both reanalyses have become worse for the spring period, compared to correlation coefficient for winter period. ERA-Interim has the best correlation coefficient at

r=0.81 [*Bromwich et al., 2015*], while the correlation coefficient to ERA5 is r=0.77. This implies that both reanalyses during the spring period do not represent the true state very well as they do to the winter period.

Respectively for the upward longwave radiation (LWU), both reanalyses have a large correlation coefficient r>0.96, where ERA5 comes out with best value. On the other hand, ERA-Interim has the best bias at 0.89 $W\ m^{-2}$, while the bias to ERA5 is 5.44 $W\ m^{-2}$. Hence both reanalyses overestimate the LWU, due to the influence the temperature has from Stefan-Boltzmann's law [*Graham et al., 2017*]. The overestimation can easily be seen in Figure 13 for ERA5. Additional Figure 16 b) display that most differences between ERA5 and observations are on the positive side in the graph, which means that the reanalysis has a higher value than the observations. In contrast ERA-Interim has more variations for the difference between reanalysis and observations from -10 $W\ m^{-2}$ to 29 $W\ m^{-2}$, where the peaks for ERA-Interim are around -4 $W\ m^{-2}$ and 0 $W\ m^{-2}$.

Both ERA5 and ERA-Interim have low values for the correlation coefficient for the net longwave radiation (LWN), ERA-Interim has the highest reaching 0.48. On the other hand, both reanalyses have a negative bias, whereas the bias to ERA5 at -5.14 $W\ m^{-2}$ much better than that of ERA-Interim at -20.42 $W\ m^{-2}$. Figure 14 distinctly show that both reanalyses underestimate the LWN [*Sotiropoulou et al., 2015*]. Therefore, a conclusion can be made that both reanalyses perform better for the LW components during the winter period than for spring, due to the increase in cloud that occurs during spring period.

Remember that the spring period takes place during polar day. Thus, shortwave radiation (SW) occurs during spring period. ERA5 has the smallest bias at 2.84 $W\ m^{-2}$ for the SWD, but ERA-Interim outperformed ERA5 for both the correlation coefficient and RMSE value see Table 2. Further the overestimation of SWD in both reanalyses proves that the reanalyses lack a certain understanding of cloud condition. Hence, both reanalyses give erroneous cloud conditions. From the timeseries Figure 13, both reanalyses capture the SWD trend for the transition between day and night. Figure 16 c) show a big variation of the differences between reanalysis and observations for both ERA5 and ERA-Interim [*Wesslén et al., 2014; Sotiropoulou et al., 2015*]. In addition, the biggest differences exist between ERA5 data and observations.

For the upward shortwave radiation (SWU), both reanalyses still capture the transition between day and night seen in Figure 13. Both reanalyses have a bias around at -17 $W\ m^{-2}$, with ERA5 having a slightly better result. A similar result is found in [*Sotiropoulou et al., 2015*] for ECMWF Integrated Forecast System (IFS). Accordingly, both reanalyses underestimate the true state for SWU. This can be seen from Figure 16 d) that the area under curves are larger on the negative side than on the positive side for both reanalyses. While both reanalyses have almost the same value for the bias, ERA-Interim does surpass ERA5 for the calculated correlation coefficient and RMSE value seen in Table 2.

Overall ERA-Interim agrees more with observations for estimating the SW, seen from the correlation coefficient for SWD, SWU and SWN. Nevertheless, ERA5 has the best bias for all three cases. Seen from the SWN timeseries Figure 14, that overall the reanalyses overestimate the true state. This indicate that less SW radiation was absorbed by the surface and as a result of this the surface albedo for both reanalyses are likely too low. In addition, Figure 16 d) indicates the same result, since the maximums values are more on the negative side. The same result has been mentioned in [*Wesslén et al., 2014*].

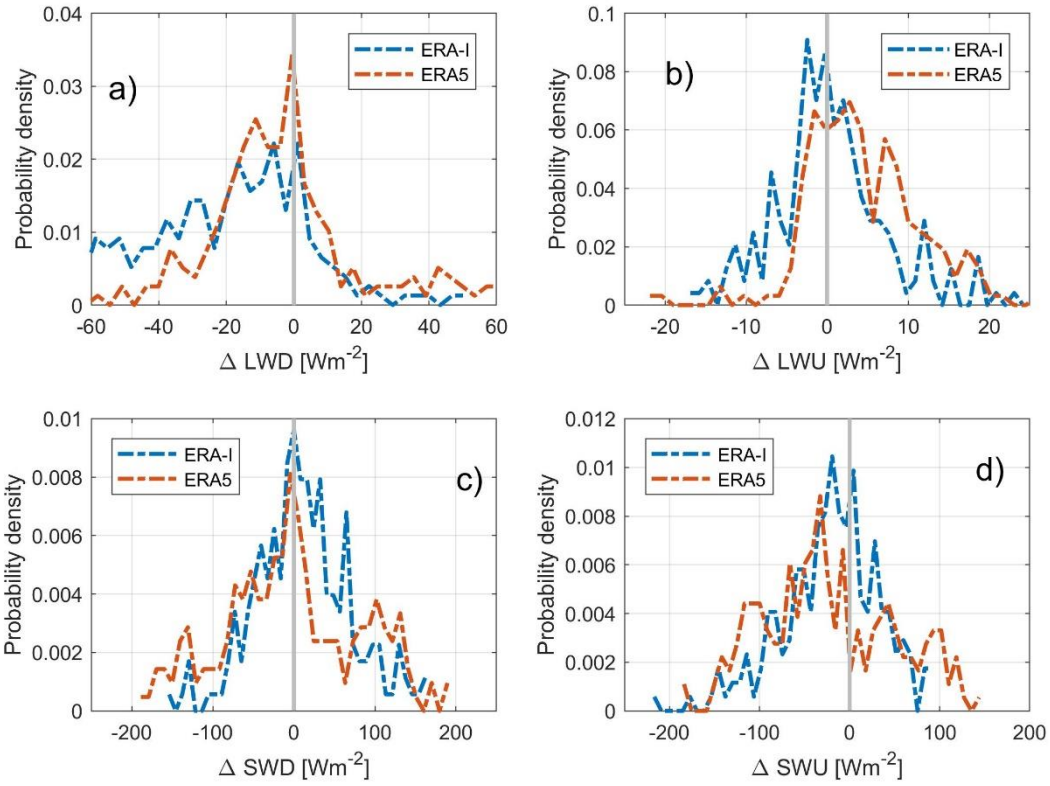

Figure 16: Probability density function (PDF) of the difference between the two reanalyses and N-ICE2015 observations for spring period. (a) downward longwave radiation in $W\ m^{-2}$, (b) upward longwave radiation in $W\ m^{-2}$, (c) downward shortwave radiation in $W\ m^{-2}$, and (d) upward shortwave radiation in $W\ m^{-2}$.

***Table 2**: Summary of model errors: mean bias, correlation coefficient and root-mean-square error (RMSE) between ERA-Interim/ERA5 and N-ICE2015 observations for the spring period (April – June). For the variables from Figure 12-13.*

Spring period				
Variable	**Model**	**Bias**	**Corr**. (no unit)	**RMSE**
T2M (℃)	ERA-I	1.42	0.9840	1.85
	ERA5	1.47	0.9817	1.96
MSLP (Pa)	ERA-I	0.66	0.9942	1.03
	ERA5	0.94	0.9966	0.95
Wind -U10M ($m\ s^{-1}$)	ERA-I	0.18	0.8493	1.80
	ERA5	-0.14	0.9493	1.03
QVI ($g\ m^{-2}$)	ERA-I	0.13	0.9627	0.86
	ERA5	0.17	0.9729	3.09
LWD ($W\ m^{-2}$)	ERA-I	-19.53	0.8122	31.95
	ERA5	0.26	0.7550	25.88
LWU ($W\ m^{-2}$)	ERA-I	0.89	0.9634	7.15
	ERA5	5.44	0.9593	9.56
LWN ($W\ m^{-2}$)	ERA-I	-20.42	0.4841	29.99
	ERA5	-5.17	0.2591	22.91
SWD ($W\ m^{-2}$)	ERA-I	14.67	0.8749	59.52
	ERA5	2.84	0.3923	176.01
SWU ($W\ m^{-2}$)	ERA-I	-17.72	0.8064	56.47
	ERA5	-17.18	0.4603	139.79
SWN ($W\ m^{-2}$)	ERA-I	32.10	0.7863	46.08
	ERA5	20.02	0.0807	54.25

4.1.3 Summary

In this section the evaluation found out that both reanalyses overestimate the near surface temperature for both periods. The overestimation for the near surface temperature mostly occurred when the temperature was quite cold. Furthermore, the upward longwave radiation was also overestimated in both reanalyses, due to the overestimation for the near surface temperature.

On one hand, the net longwave radiation is overestimated in both reanalyses because of the overestimation for the upward longwave radiation during winter period. On the other hand, the net longwave radiation underestimates the true state in both reanalyses during the spring period. The underestimation of net longwave radiation is due to the underestimation of the downward longwave radiation. Moreover, that the downward longwave radiation underestimates in both reanalyses are due fact that the reanalyses can present cloud conditions very well.

The spring period is most interesting to look at for the shortwave radiation. Again, the clouds have a direct effect on a variable in the reanalyses. The downward shortwave radiation overestimates the true state in the reanalyses, due to the fact some of the downward shortwave radiation is absorbed by the cloud in the real world. Moreover, the net shortwave radiation is also overestimated in the reanalysis, which implies that that both reanalyses have a to low surface albedo.

At last, both reanalyses represent the mean sea level pressure and the water vapor path remarkably well.

4.2 Evaluation of the forecast model to the ERA-Interim reanalysis

This section in the thesis will look closely at how the assimilated N-ICE2015 observations affect the reanalyses values from ERA-Interim. Hence, the difference between the forecast model value and reanalysis value for N-ICE2015 locations and other locations are compared with each other. Thus, the evaluation will still take place during the N-ICE2015 period, and the period will still be separated into winter and spring period. In addition, another reference point in the evaluation will be obtained reanalysis data from 11 other locations that will be outside the boundary from where N-ICE2015 took place in the reanalysis. The other locations will follow along the same path as the N-ICE2015 expedition, but will have +1 latitude degree (farther north) and from -5 to +5 degree differences in longitude (farther east or west). Hence, the smallest difference between the other location and N-ICE2015 locations will be about 111.2 km.

As mentioned before for this evaluation will look at the difference between the different reanalysis variables and different forecast model variables for the two locations. The two locations are defined as the N-ICE2015 expedition locations and second would be the mean of the 11 other locations. The difference that is looked at is the difference between the reanalysis value for a given timestep and value from the forecast model that has run for 12 hours. Hence, both values are obtained from the same timestep. The difference will be the reanalyses value subtracted with the forecast value, as seen in equation below.

$$Diff = Reanalysis - Forecast\ model$$

Additionally, remark for evaluating the wind speed components. As mentioned before the wind speed measurements from N-ICE2015 are not sent for assimilation in reanalyses. Instead, the evaluation will see if the assimilated observations from N-ICE2015, such as temperature and pressure have had an effect on the reanalysis data for the wind speed variables.

The hypothesis for this evaluation is that larger differences between reanalyses and forecast model will occur for the N-ICE2015 locations, while the other locations will have smaller differences between reanalysis and forecast model. The N-ICE2015 locations will have larger values, because of the assumption that the assimilated observations from N-ICE2015 will have an effect in the assimilation process for the ERA-Interim reanalysis.

4.2.1 Winter period

The winter period as mentioned before is from the beginning of the N-ICE2015 expedition in January to the end of March. Table 3 show all the calculated biases and Root Mean Square Errors (RMSE) for the difference between reanalysis and 12-hour forecast, during the winter period for the meteorological variables 2m temperature (T2m), mean sea level pressure (MSLP), and both components to the wind speed (U10m=east-west, V10m=north-south). Further shown in Figure 17 is the probability density function for the difference between reanalysis and 12-hour forecast for the variables mentioned above.

Regarding the near surface temperature, seen in Figure 17 that the temperature differences between ERA-Interim and 12-hour forecast span from -6 ℃ to 6 ℃, and most the differences are centred between -2 ℃ and 2 ℃ for the N-ICE2015 locations and the other locations. The same result is found in [*Sotiropoulou et al., 2015*] for three cloud scheme forecasts. Furthermore, Figure 17 show that other locations have the largest peak near 0 ℃. Hence, the other locations have smaller differences between ERA-Interim and 12-hour forecast, than the differences between ERA-Interim and 12-hour forecast for the N-ICE2015 locations. In addition, both N-ICE2015 locations and other locations have two peaks near -0.5 ℃ and -1.5 ℃, but the other locations have highest probability density for both peaks.

N-ICE2015 locations have the smallest bias at -0.49 ℃, but the bias from the other locations are only 0.01 ℃ larger at -0.5 ℃. Thus, both biases are close to the highest peak shown in Figure 17 for both locations. Moreover, the negative biases imply that the 12-hour forecast values are at average larger than the ERA-Interim reanalysis values. This is also confirmed in [*Sotiropoulou et al., 2015*], where three different cloud schemes overestimated the true state

during the ASCOS field campaign. Consequently, the result of negative biases also agrees with [*Tjernström and Graversen et al., 2009*] that the reanalysis is consistently colder than the forecast model temperature in this case after assimilating the observations from SHEBA. As a result, from this can a conclusion be made that the reanalysis temperature value is consistently smaller (colder) than the 12-hour forecast temperature value, after the assimilating the temperature observations from N-ICE2015.

In addition, the conclusion can further be proven from Figure 17. The areas under the curves for both N-ICE2015 locations and other locations are larger on the negative side for the temperature differences. This implies that most differences between ERA-Interim and 12-horu forecast are negative. Hence, the 12-hour forecast has a larger value than the value for ERA-Interim. The result of this, may be the reason for the temperature overestimation in ERA-Interim seen in section 4.1.1, since the forecast model has been used in the assimilation process for obtaining the reanalysis value.

Furthermore, the deviation between the RMSE values for both locations are small. The other locations have the smallest RMSE value at 2.49 ℃, while the RMSE value for N-ICE2015 locations are slightly larger at 2.56 ℃.

Thus, the N-ICE2015 observations have had an effect on ERA-Interim, because that they were assimilated into the reanalysis from the radiosondes. Due to the fact that the larger temperature differences between ERA-Interim and 12-hour forecast value occurs for N-ICE2015 locations, compared to the smaller temperature differences for the other locations. In addition, the RMSE value is also slightly larger for the N-ICE2015 locations.

Concerning the mean sea level pressure, Figure 17 show that the curves for both N-ICE2015 locations and the other locations have differences from -500 *Pa* to 400 *Pa*. Further, Figure 17 show that the other locations have the closest peak near 0 *Pa*, but the N-ICE2015 locations have the highest peak near 40 *Pa.* On the other hand, the probability density values are quite small for both peaks. Both curves are similar in Figure 17, and it is hard to tell on which side of 0 *Pa* the area under the curve is larger. The biases from Table 3 implies that the area is slightly larger on the positive side, due to the positive value for the bias. The other locations have the smallest bias at 3.88 *Pa,* while the bias for N-ICE2015 locations are larger at 7.37 *Pa*. Overall, the positive biases implies that the 12-hour forecast value is smaller than the ERA-Interim value.

In addition, the other locations have the smallest RMSE value at 423 *Pa*, which implies a slightly better correlation between the ERA-Interim and the 12-hour forecast compared to the N-ICE2015 locations that have a RMSE at 431 *Pa*.

The calculated biases and RMSE values from Table 3 may imply that the assimilations of the N-ICE2015 pressure observations from the radiosondes have had an effect on the reanalysis ERA-Interim. On the other hand, it is quite hard to make this conclusion out from Figure 17 alone. On the other hand, the forecast model for the pressure value presents the mean sea level pressure fairly well. Similar result for the pressure has been found in [*de Boer et al., 2014*].

Regarding the east-west wind speed (U10m), the bias for the other locations are surprisingly low at 0.01 $m\ s^{-1}$, while the bias for N-ICE2015 locations are negative at -0.23 $m\ s^{-1}$. From Figure 17, the other locations have two high peaks, one at 0.5 $m\ s^{-1}$, while the highest is around 1.2 $m\ s^{-1}$. Similarly, the N-ICE2015 locations have two peaks around -0.5 $m\ s^{-1}$ and 0.7 $m\ s^{-1}$. The curves for both N-ICE2015 locations and other locations are quite similar to each other, as seen in Figure 17. Both curves have a high peak near 0 $m\ s^{-1}$. In addition, the bias for N-ICE2015 locations imply that a larger amount of the 12-hour forecast values is larger, than the values for ERA-Interim.

The wind speed observations from the N-ICE2015 expedition are not assimilated into the reanalyses. On the other hand, the other assimilated observations from N-ICE2015 may have had an effect on the reanalysis data from ERA-Interim. The RMSE values from Table 3 are what the hypothesis expects for them to be. Hence, the other locations have a smaller RMSE value at 2.2 $m\ s^{-1}$, while N-ICE2015 locations have the largest at 2.42 $m\ s^{-1}$.

From the calculated biases, RMSE values and slightly from what is shown in Figure 17, the conclusion is that the assimilated observations from N-ICE2015 have an effect on the reanalysis data for ERA-Interim. Even if the wind speed observations are not used into the assimilation process, the assimilated variables such as temperature and pressure have had an effect on the reanalysis values. On the other hand, the forecast model can probably represent the east-west wind speed quite well because of the small bias for the difference between ERA-Interim and 12-hour forecast, according to [*de Boer et al., 2014; Sotiropoulou et al., 2015*].

Furthermore, the same can not be said for the north-south wind speed (V10m). The biases and RMSE values from Table 3 give the expected result, that the other locations have better

values for the mean bias and RMSE value compared to the N-ICE2015 locations. The N-ICE2015 locations have the largest bias at -0.5 $m\ s^{-1}$ and RMSE at 2.44 $m\ s^{-1}$, while the other locations bias is smaller at -0.37 $m\ s^{-1}$ and RMSE is insignificant smaller at 2.42 $m\ s^{-1}$.

On the other hand, Figure 17 show that the N-ICE2015 locations has the highest peak near 0 $m\ s^{-1}$, and this peak is much larger than the peak for the other locations. Consequently, the results from the mean bias and RMSE value imply that the wind speed observations from N-ICE2015 are assimilated into the reanalysis, which is confirmed in [*Graham et al., 2017*].

***Table 3**: Summary of model errors: mean bias, and root-mean-square error (RMSE) between ERA-Interim reanalysis and the 12-hour forecast. For the variables from Figure 17.*

Winter period			
Variable	**Location**	**Mean bias**	**RMSE**
T2M (℃)	N-ICE	-0.49	2.56
	Other	-0.50	2.49
MSLP (Pa)	N-ICE	7.37	431.8
	Other	3.88	423.8
U10m ($m\ s^{-1}$)	N-ICE	-0.23	2.42
	Other	0.01	2.20
V10m ($m\ s^{-1}$)	N-ICE	-0.50	2.44
	Other	-0.37	2.42

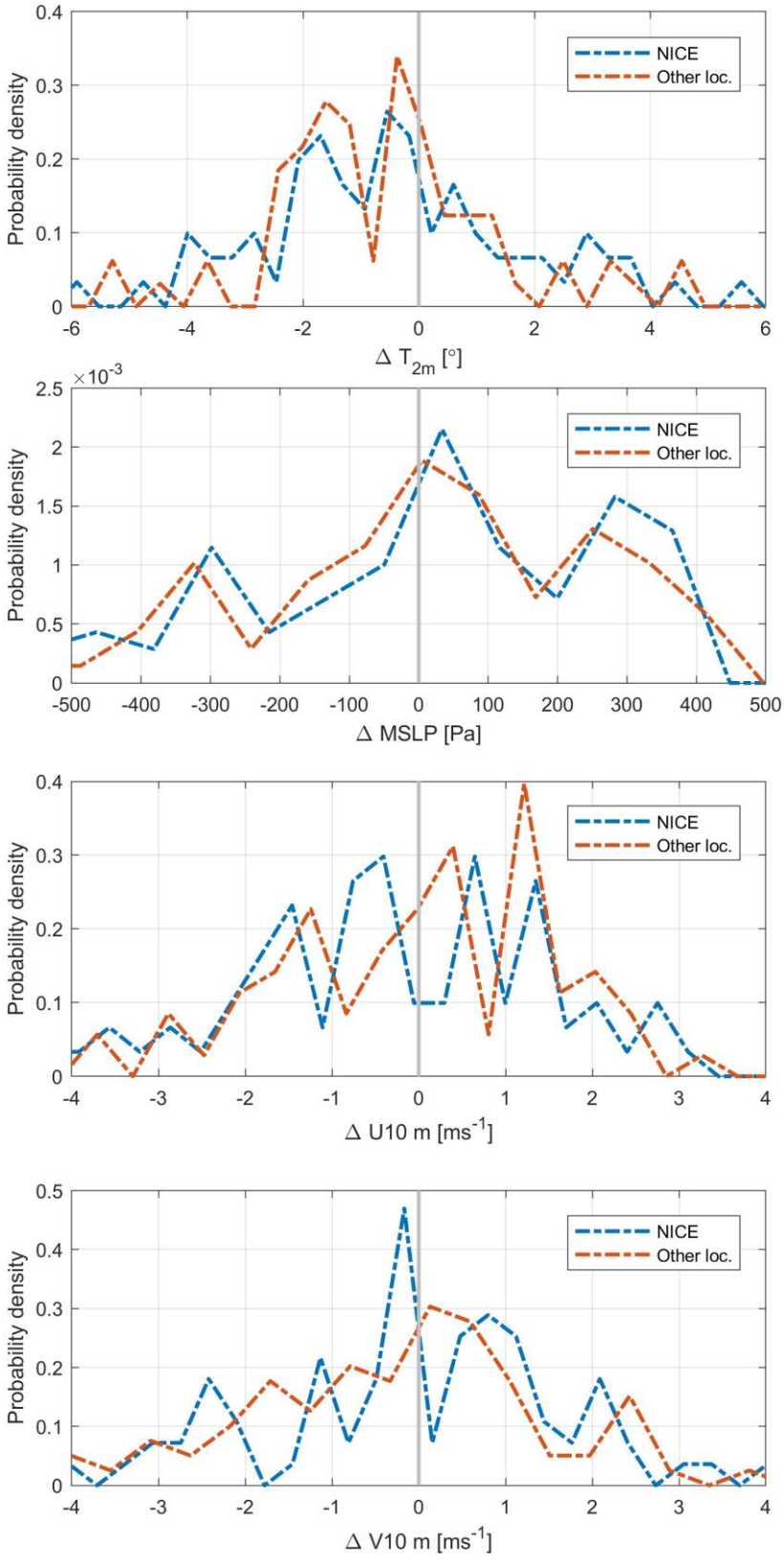

Figure 17: Probability density functions between ERA-Interim reanalysis and 12-hour forecast for all variables during the winter period. Comparing N-ICE2015 location (blue) and other locations (red). From top to bottom: 2m temperature T2m, mean sea level pressure MSLP (Pa), wind speed (east – west) U10m $(m\ s^{-1})$ and wind speed (north – south) V10m $(m\ s^{-1})$.

4.2.2 Spring period

The spring period will still be the same from the period April to June during the N-ICE2015 expedition. Table 4 show all the calculated biases and Root Mean Square Errors (RMSE) for the difference between reanalysis and 12-hour forecast, during the winter period for the meteorological variables 2m temperature (T2m), mean sea level pressure (MSLP), and both components to the wind speed (U10m=east-west, V10m=north-south). Further shown in Figure 18 is the probability density function for the difference between reanalysis and 12-hour forecast for the variables mentioned above.

Considering the near surface temperature, in Table 4 both N-ICE2015 locations and other locations have a positive mean bias. As expected the other locations have a smaller bias at 0.2 ℃, while the bias for N-ICE2015 locations are larger at 0.52 ℃. Overall, the biases imply that most of the 12-hour forecast values are smaller compared to the ERA-Interim reanalysis value. Hence, the spring period has the opposite result than the result found for the winter period. A result from this can be the slightly smaller bias that came as a result in section 4.1.2 for the spring period. In addition, the positive biases for the spring period are not consistent with the result in [*Tjernström and Graversen et al., 2009*], where the conclusion was that the reanalysis is consistent colder than the forecast model during the period when the observations are assimilated into the reanalysis.

On the other hand, Figure 18 show that most temperature difference between ERA-Interim and 12-hour forecast are centred between -1 ℃ and 1 ℃, and the overall range of the differences are between -3 ℃ and 3 ℃. Similar result is found in [*Sotiropoulou et al., 2015*]. In addition, the differences values for spring period between ERA-Interim and 12-hour forecast are relatively smaller than the differences values for the winter period. It is displayed in Figure 18 that the other locations have the closest peak near 0 ℃, and the highest peak around 0.5 ℃. In addition, the other locations have a higher probability density centred near zero difference, and implies that the N-ICE2015 locations have larger valued for the differences.

Moreover, the RMSE values in Table 4 have the same result that fits the hypothesis. The N-ICE2015 locations have the largest RMSE value at 1.37 ℃, while the RMSE value for the other locations are smaller at 1.06 ℃.

Thus, the conclusion is that the assimilated observations from N-ICE2015 have influenced the reanalysis data for ERA-Interim. This result is anticipated because it is coexistent with the result for the near surface temperature during winter period, and a change in season should not affect the result.

Regarding the mean sea level pressure, Figure 18 show that the most differences between ERA-Interim and the 12-hour forecast for both N-ICE2015 locations and the other locations are centred between -200 *Pa* and 200 *Pa.* Same as for the winter period, during the spring period the N-ICE2015 locations have the closest peak near 0 *Pa*. Further seen in Figure 18, the N-ICE2015 locations have an additional peak near -80 *Pa*. On the other hand, the other locations have the highest peak on the positive side in the graph at 30 *Pa*.

Surprisingly, the other locations have a large negative bias at -35.69 *Pa*, which implies that most values for the 12-hour forecast are larger than the values for the reanalysis. Even more surprisingly, the bias for the N-ICE2015 locations are smallest at -33.86 *Pa*. Furthermore, the N-ICE2015 locations have the smallest RMSE values, seen in Table 4. The negative biases for both locations implies that the 12-hour forecast values are overall larger compared to the ERA-Interim reanalysis values.

Unsurprisingly, it is quite difficult to deduce from the results if there exist an effect on the reanalysis data due to the assimilation of the pressure observations from N-ICE2015 expedition. The result from the calculated variables and Figure 18 implies that the assimilated observations had a minimal effect on the reanalysis. On the other hand, the result suggest that the forecast models are relatively good to simulate the mean sea level pressure during this period, because of the reasonable low biases and RMSE values.

Next, in the line is the evaluation of the east-west wind speed during the spring period. Figure 18 show that the other locations have a highest peak around -0.4 $m\ s^{-1}$, while the highest peak for the N-ICE2015 locations are near 0.3 $m\ s^{-1}$. For both N-ICE2015 locations and the other locations are the differences between ERA-Interim and 12-hour forecast centred between -2 $m\ s^{-1}$ and 2 $m\ s^{-1}$. Furthermore, both N-ICE2015 locations and the other locations have a negative bias, where the bias for the other locations are the smallest as

expected. The bias for N-ICE2015 locations are at -0.16 $m\ s^{-1}$ and the bias for other locations are -0.10 $m\ s^{-1}$. The small biases for the east-west wind speed are also confirmed in [*de Boer et al., 2014*].

On the other hand, N-ICE2015 locations have the smallest RMSE value at 1.28 $m\ s^{-1}$, while the other locations have a slightly larger RMSE value at 1.35 $m\ s^{-1}$. Thus, make it difficult to decide if the assimilated N-ICE2015 observations have had an effect on the reanalysis data for the east-west wind speed variable for ERA-Interim. Nevertheless, due to the biases and slightly higher probability density for the other locations near 0 $m\ s^{-1}$ in Figure 18, the conclusion will be that assimilation of the N-ICE2015 measurements have influenced the reanalysis data for the east-west wind speed for ERA-Interim.

Finally, for the north-south wind speed (V10m), the graph for the spring period in Figure 18 is similar to the graph for the winter period in Figure 17. N-ICE2015 locations have a much larger peak near 0 $m\ s^{-1}$ difference, than what the other locations have. For both N-ICE2015 locations and the other locations are the differences between ERA-Interim and 12-hour forecast centred between -2.5 $m\ s^{-1}$ and 2 $m\ s^{-1}$.

As anticipated, the other locations have smaller mean bias and RMSE value, where the bias is -0.29 $m\ s^{-1}$ and the RMSE is 1.61 $m\ s^{-1}$. For the N-ICE2015 locations are the bias larger at -0.41 $m\ s^{-1}$ and have a larger RMSE value at 1.72 $m\ s^{-1}$. The small biases for the north-south wind speed are also found in [*de Boer et al., 2014*].

From the calculated mean bias and RMSE values, we will deduce that assimilating the N-ICE2015 observations have influenced the reanalysis data for north-south wind speed for ERA-Interim. Granted the conclusion can not be made by only using the graph in Figure 18.

***Table 4**: Summary of model errors: mean bias, and root-mean-square error (RMSE) between ERA-Interim reanalysis and the 12-hour forecast. For the variables from Figure 18.*

Spring period			
Variable	**Location**	**Mean bias**	**RMSE**
T2M (℃)	N-ICE	0.52	1.37
	Other	0.20	1.06
MSLP (Pa)	N-ICE	-33.86	144.4
	Other	-35.69	147.2
U10m ($m\ s^{-1}$)	N-ICE	-0.16	1.28
	Other	-0.10	1.35
V10m ($m\ s^{-1}$)	N-ICE	-0.41	1.72
	Other	-0.29	1.61

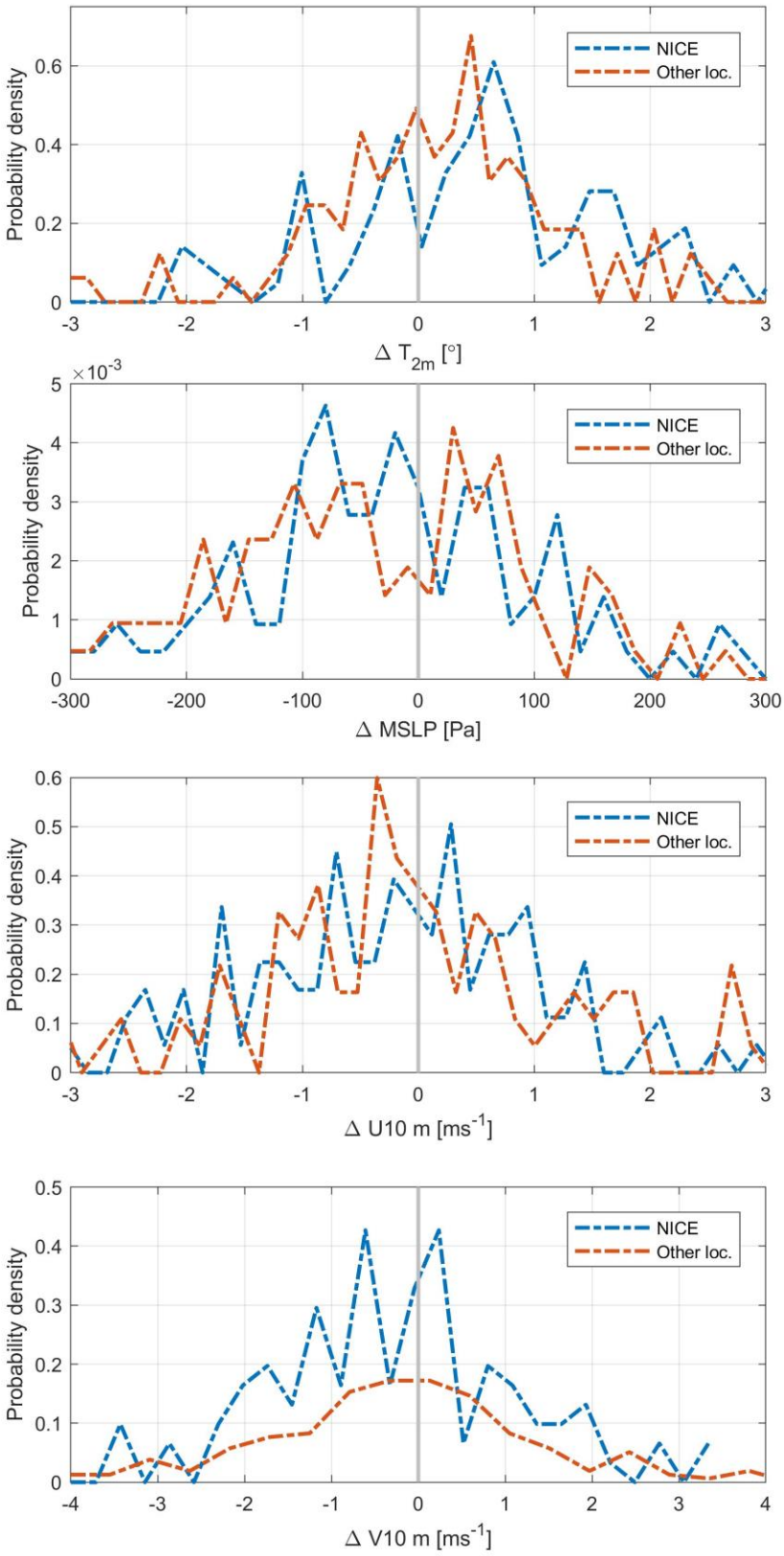

Figure 18: Probability density functions between ERA-Interim reanalysis and 12-hour forecast for all variables during the spring period. Comparing N-ICE2015 location (blue) and other locations (red). From top to bottom: 2m temperature T2m, mean sea level pressure MSLP (Pa), wind speed (east – west) U10m $(m\ s^{-1})$ and wind speed (north – south) V10m $(m\ s^{-1})$.

4.2.3 Summary

This section was assigned for examine if the assimilated N-ICE2015 observations had influenced the reanalysis data by looking at differences between ERA-Interim and the 12-hour forecast for the N-ICE2015 locations and mean of 11 other locations. The result found in this section suggest that the ERA-Interim reanalyses data were affected by the assimilated N-ICE2015 observations for all variables.

4.3 Evaluation of the forecast model to the ERA5 reanalysis

This section will be similar to section 4.2, but will instead focus on the newest reanalysis ERA5. Hence, the difference between ERA5 and the 12-hour forecast for the N-ICE2015 locations and the other locations will be evaluated.

The ERA5 reanalysis as mentioned before has a horizontal grid resolution at 31 *km*. Thus, the other locations have that the nearest locations are around 111 *km* away from the N-ICE2015 locations, which will be grid points away. Moreover, the hypothesis implies that clearer difference between the N-ICE2015 location and the other locations should be seen.

4.3.1 Winter period

The winter period as mentioned before is from beginning of the N-ICE2015 expedition in January to the end of March. Table 5 show all the calculated biases and Root Mean Square Errors (RMSE) for the difference between reanalysis and 12-hour forecast, during the winter period for the meteorological variables 2m temperature (T2m), mean sea level pressure (MSLP), and both components to the wind speed (U10m=east-west, V10m=north-south). Further shown in Figure 19 is the probability density function for the difference between reanalysis and 12-hour forecast for the variables mentioned above.

Considering the near surface temperature, the differences overall between ERA5 and 12-hour forecast are much smaller, than the differences found in section 4.2.1 between ERA-Interim and 12-hour forecast. Figure 19 show that the temperature differences between ERA5 and 12-hour forecast are centred between -0.05 ℃ and 0.05 ℃ for the other locations, while for N-ICE2015 locations are the differences centred between -0.05 ℃ and 0.1 ℃. In addition, the other locations have the highest peak that is closest to 0 ℃ difference.

Both the N-ICE2015 locations and the other locations have remarkably small biases, where the largest bias at 0.03 ℃ is for the N-ICE2015 locations, and the other location have a bias at -0.01 ℃. Thus, it is not possible to proclaim that the reanalysis is consistently colder than the forecast model temperature after assimilating the N-ICE2015 observations, as is done in

[*Tjernström and Graversen et al.,* 2009]. Furthermore, not anticipated the other locations have the largest RMSE value at 0.11 ℃, while the N-ICE2015 locations RMSE value is 0.06 ℃ smaller at 0.05 ℃.

On the other hand, Figure 19 clearly show that for the other location most differences between ERA5 and 12-hour forecast are situated close to zero, because of the large probability density value, compared to the lesser probability density value for the N-ICE2015 locations around 0 ℃. Thus, the results imply that the assimilation of the temperature observations from N-ICE2015 expedition have influenced the reanalysis data in ERA5.

Regarding the mean sea level pressure, Figure 19 show that the N-ICE2015 locations have the largest peak around -10 *Pa,* which is the closest peak near 0 *Pa.* The difference between ERA5 and 12-hour forecast span from -100 *Pa* to 100 *Pa* for both the other locations and N-ICE2015 locations. Both N-ICE2015 locations and the other locations have a negative bias, where as anticipated the other locations have the smallest bias at -1.27 *Pa,* and N-ICE2015 locations have a larger bias at -4.02 *Pa*. These biases are smaller compared to the biases found in section 4.1.1 for ERA-Interim.

On the other hand, the one location that has the smallest RMSE value are the N-ICE2015 locations which seen from Table 5 and the RMSE is 54.22 *Pa*, while the other locations have a RMSE value at 58.91 *Pa*.

That the smallest differences between ERA5 and 12-hour forecast have a larger probability density value for N-ICE2015 locations, imply that the assimilated pressure observation from N-ICE2015 have not had an effect on the reanalysis data for ERA5. Nevertheless, that the other locations have the smallest bias will imply that the assimilated pressure observation from N-ICE2015 have influenced the reanalysis data for ERA5. Hence, the results suggest that the assimilation of the pressure observations from N-ICE201 expeditions have had a slight effect on the reanalysis data for ERA5. Furthermore, the forecast model for the pressure value present the mean sea level pressure fairly well, as seen for ERA-Interim in section 4.1.1. Similar result for the pressure has been found in [*de Boer et al., 2014*].

Next, regarding the east-west wind speed, from Figure 19 most differences for both N-ICE2015 locations and the other locations between ERA5 and 12-hour forecast are centred

between -0.5 $m\ s^{-1}$ and 0.5 $m\ s^{-1}$. Figure 19 show a clear distinction for the two locations N-ICE2015 locations and the other locations. The other locations have the highest peak near 0.2 $m\ s^{-1}$, and the overall area under curve near 0 $m\ s^{-1}$ is largest for the other locations, then for the N-ICE2015 locations. Hence, more differences between ERA5 and 12-hour forecast are smaller for the other locations.

On one hand, the difference between the biases for the two locations are only 0.01 $m\ s^{-1}$, where the N-ICE2015 locations have the smallest bias at -0.05 $m\ s^{-1}$. On the other hand, the other locations have the smallest RMSE value 0.48 $m\ s^{-1}$, while the RMSE value for N-ICE2015 locations are at 0.6 $m\ s^{-1}$. Accordingly, because of the small deviation between the N-ICE2015 locations and the other locations for the calculated mean biases and RMSE values and the clear distinction shown in Figure 19 between the two locations, the conclusion would be that the assimilated N-ICE2015 observations have had an effect on the reanalysis data for east-west wind for ERA5.

Finally, north-south wind is only variable left. Similarly, to the east-west wind the other locations for the north-south wind have the largest bias at -0.06 $m\ s^{-1}$ and the smallest RMSE at 0.48 $m\ s^{-1}$, seen in Table 5. According to [*de Boer et al., 2014; Sotiropoulou et al.,* 2015], the small bias for the difference between reanalysis and forecast model implies that the forecast model for ERA5 represent the wind speed quite well. Further, Figure 19 show that the other locations have the highest peak near 0 $m\ s^{-1}$. Hence, the results insinuate that the assimilated observations from N-ICE2015 expedition have had an influence on the reanalysis ERA5.

***Table 5**: Summary of model errors: mean bias, and root-mean-square error (RMSE) between ERA5 reanalysis and the 12-hour forecast. For the variables from Figure 19.*

Winter period			
Variable	**Location**	**Mean bias**	**RMSE**
T2M (℃)	N-ICE	0.03	0.05
	Other	-0.01	0.11
MSLP (Pa)	N-ICE	-4.02	54.22
	Other	-1.27	58.91
U10m ($m\ s^{-1}$)	N-ICE	-0.05	0.60
	Other	-0.06	0.48
V10m ($m\ s^{-1}$)	N-ICE	0.03	0.88
	Other	-0.06	0.54

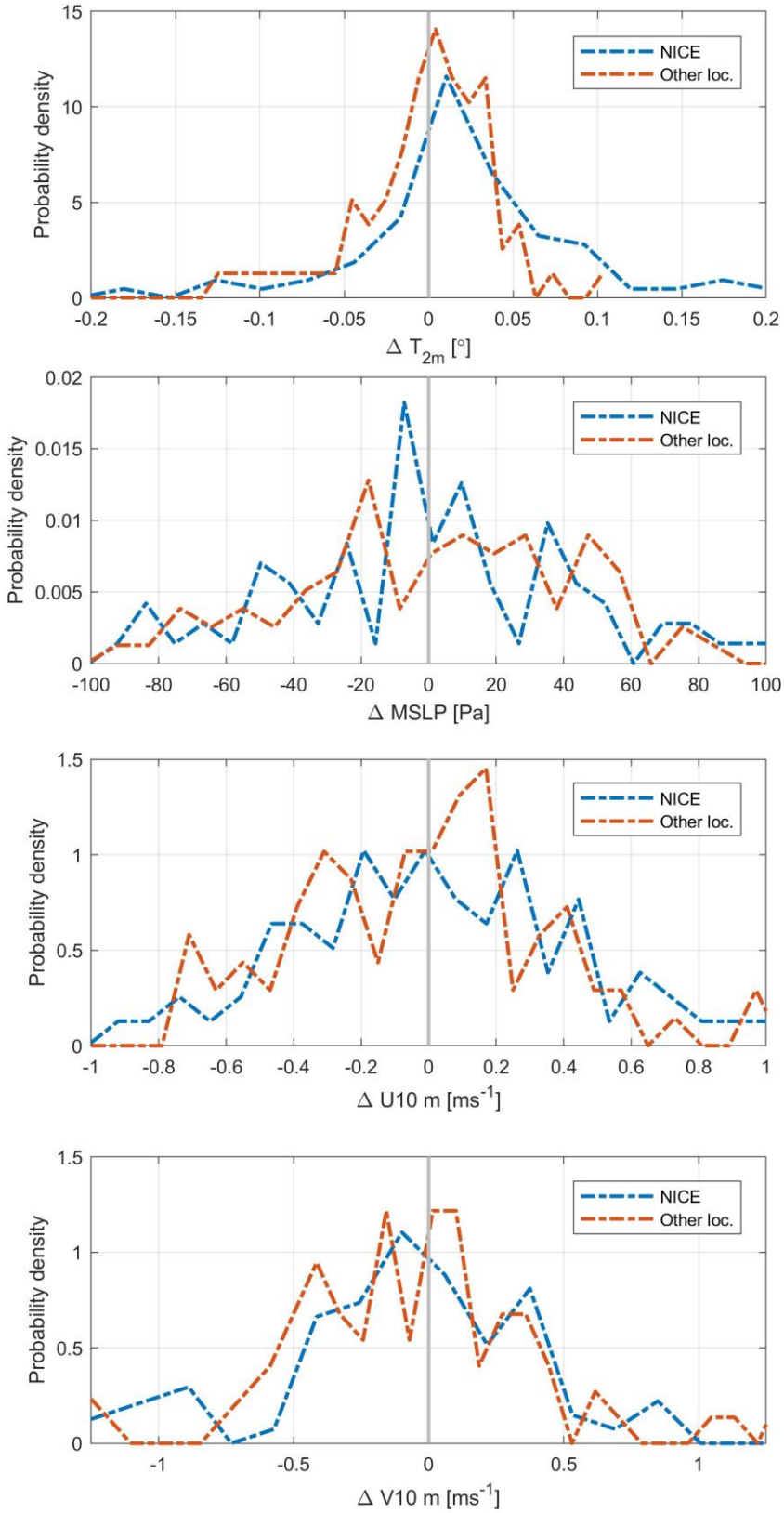

Figure 19: Probability density functions between ERA5 reanalysis and 12-hour forecast for all variables during the winter period. Comparing N-ICE2015 location (blue) and other locations (red). From top to bottom: 2m temperature T2m, mean sea level pressure MSLP (Pa), wind speed (east – west) U10m ($m\ s^{-1}$) and wind speed (north – south) V10m ($m\ s^{-1}$).

4.3.2 Spring period

The spring period will still be the same from the period April to June during the N-ICE2015 expedition. Table 5 show all the calculated biases and Root Mean Square Errors (RMSE) for the difference between reanalysis and 12-hour forecast, during the winter period for the meteorological variables 2m temperature (T2m), mean sea level pressure (MSLP), and both components to the wind speed (U10m=east-west, V10m=north-south). Further shown in Figure 20 is the probability density function for the difference between reanalysis and 12-hour forecast for the variables mentioned above.

Regarding the near surface temperature, a clear distinction between the N-ICE2015 locations and the other locations are shown in Figure 20. The other locations have a much higher probability density value for differences between ERA5 and 12-hour forecast near 0 ℃, then the differences between ERA5 and 12-hour forecast for the N-ICE2015 locations. In addition, the biases and RMSE values from both locations are almost equal, seen in Table 6. The difference between the calculated variables for the two locations are for the mean bias at 0.003 ℃ and for the RMSE value at 0.02 ℃.

As a result, from the small differences in the calculated variables for the two locations and the clear distinction shown in Figure 20, will the conclusion be that the assimilated temperature observations from N-ICE2015 have had a clear effect on the reanalysis ERA5.

Considering the mean sea level pressure, the N-ICE2015 locations have the smallest bias at -14.52 *Pa*, while the other locations have a slightly larger bias at -14.70 *Pa*. Figure 20 show that curves for the both N-ICE2015 locations and the other locations are quite alike. The area under the curves are larger on the negative side of 0 *Pa* for both locations. In addition, the other locations have larger probability density for differences between ERA5 and 12- hour forecast near 0 *Pa*. Hence, the results still imply for the same conclusion that the assimilated N-ICE2015 observations have influenced the reanalysis data for ERA5.

Further the conclusion is also extended to the east-west wind speed. The deviation between the calculated variables for the two locations are very small. The mean biases have a difference of 0.05 $m\ s^{-1}$, and difference for RMSE values are at 0.03 $m\ s^{-1}$ between the two locations. On one hand, the N-ICE2015 locations have the smallest value for both the mean bias and the RMSE. On the other hand, the other locations have the highest peaks closest to 0 $m\ s^{-1}$. As a result, from this the assimilated observations from N-ICE2015 may have had a slight effect on the reanalysis, but the effect is not as large compared for the near surface temperature variable.

At last for the north-east wind speed, Figure 20 show similar result that was found for in section 4.2.2 for the ERA-Interim reanalysis. In addition, similarly seen for the east-west wind are the calculated mean biases and RMSE values almost the same for both N-ICE2015 location and the other locations. Therefore, the results from Table 6 imply that the assimilated N-ICE2015 observations may have had a slight effect on the reanalysis data for the north-south wind speed for ERA5.

***Table 6**: Summary of model errors: mean bias, and root-mean-square error (RMSE) between ERA5 reanalysis and the 12-hour forecast. For the variables from Figure 20.*

Spring period			
Variable	**Location**	**Mean bias**	**RMSE**
T2M (℃)	N-ICE	-0.002	0.04
	Other	0.001	0.02
MSLP (Pa)	N-ICE	-14.52	33.72
	Other	-14.70	32.86
U10m ($m\ s^{-1}$)	N-ICE	0.01	0.39
	Other	-0.04	0.33
V10m ($m\ s^{-1}$)	N-ICE	-0.04	0.36
	Other	-0.02	0.32

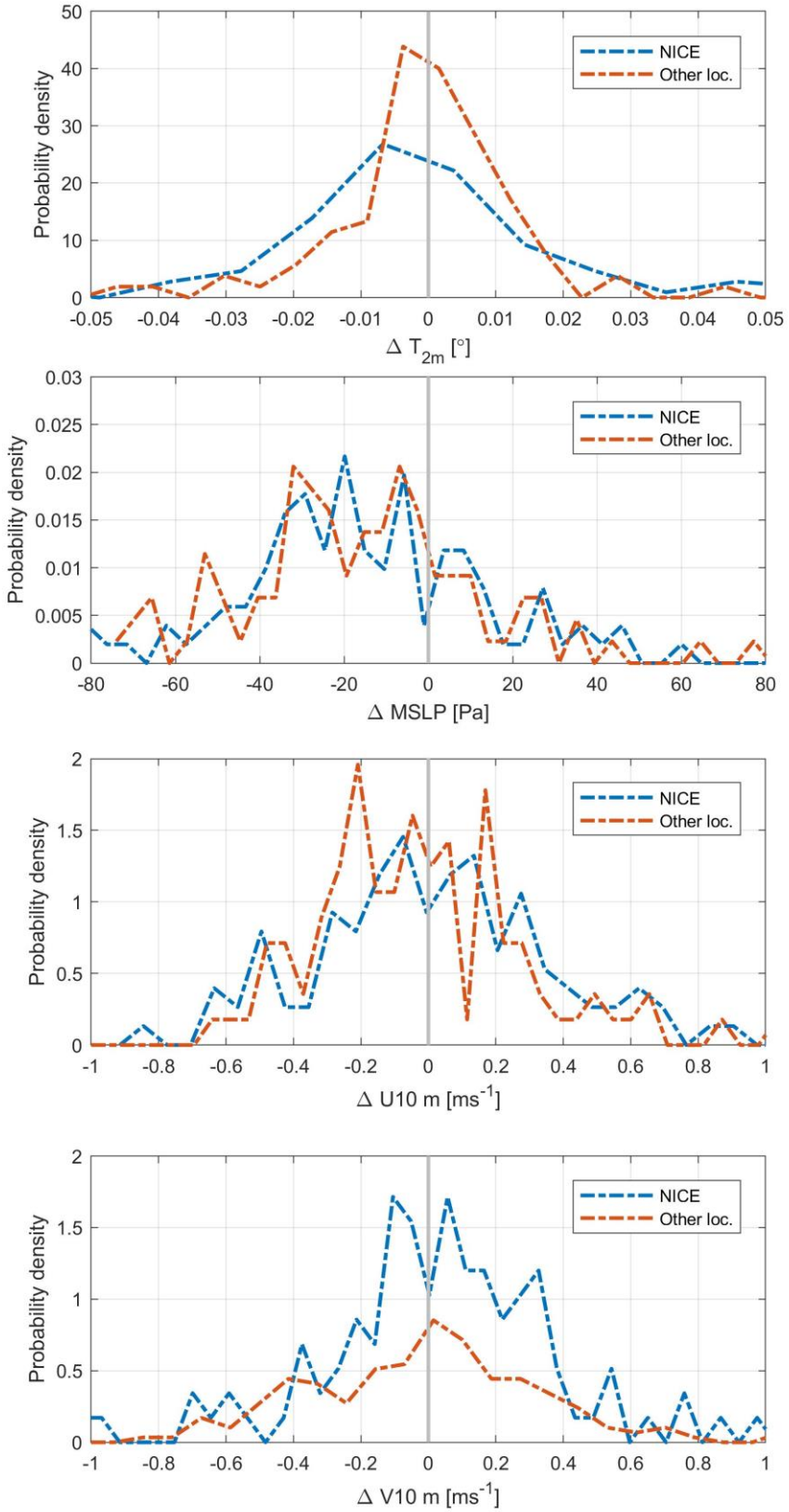

Figure 20: Probability density functions between ERA5 reanalysis and 12-hour forecast for all variables during the spring period. Comparing N-ICE2015 location (blue) and other locations (red). From top to bottom: 2m temperature T2m, mean sea level pressure MSLP (Pa)*, wind speed (east – west) U10m* $(m\ s^{-1})$ *and wind speed (north – south) V10m* $(m\ s^{-1})$.

4.3.3 Summary

This section was assigned for examine if the assimilated N-ICE2015 observations had influenced the reanalysis data by looking at differences between ERA5 and the 12-hour forecast for the N-ICE2015 locations and mean of 11 other locations. The differences between ERA5 and the 12-hour forecast were overall smaller for all variables, than the differences found in section 4.1. Similar to section 4.1 the result found in this section suggest that the ERA5 reanalyses data were affected by the assimilated N-ICE2015 observations for all of the variables.

5 Discussion

This study has focused on the evaluation of the two reanalyses ERA-Interim and ERA5 with the use of the observations from the N-ICE2015 field campaign, that lasted from middle of January to the middle of June North for Svalbard. Hence, one of the objective in this thesis was to find out how accurate the reanalyses ERA-Interim and ERA5 are in representing the measurements from N-ICE2015. In addition, another objective was to see if there was some improvement in the new reanalysis ERA5 compared to the Era-Interim reanalysis representing the previous generation of reanalyses. Furthermore, the study has concentrated on what effect the assimilated N-ICE2015 observations have on the two reanalyses ERA-Interim and ERA5, by comparing the reanalyses with the forecast model. First, there will be a discussion about the result found from the comparison between the reanalyses and observations from N-ICE2015. Additionally, remarks about improvement for ERA5 will come as the different variables are discussed. At last, there will be a discussion about the result found from the analysis of the what effect assimilated N-ICE2015 observation have on the reanalyses.

Regarding the comparison between the two reanalyses and observations from N-ICE2015, the smaller values in spring compared to those in winter for the correlation coefficient of all variables except wind are consistent with the conclusion of Lindsey et al 2014. Furthermore, the result found in section 4.1.1 and 4.1.2 suggested that both reanalyses did overestimate the near surface temperature during both winter and spring period. This phenomenon has been seen in other previous studies [e.g. *Jakobsen et al., 2012; Lindsey et al., 2014; Wesslén et al., 2014*] for the ERA-Interim reanalysis, and proceeded to exist in the latest reanalysis ERA5. In addition, the upward longwave radiation overestimates the true state both in the ERA-Interim and the ERA5 reanalysis, because of the strong relation between the near surface temperature and upward longwave radiation, due to Stefan-Boltzmann law. The overestimation of upward longwave radiation occurs during both the winter and spring periods. In the winter period the overestimation of near surface temperature and upward longwave radiation occurs especially when the temperature is below -20 ℃. In addition, the ERA-Interim reanalysis presents these two variables better than does the ERA5 reanalysis, when the temperature is below -20 ℃. On the other hand, ERA5 performs better than ERA-Interim during the spring period when the temperature is above -3 ℃.

Another problem that the reanalyses have during the winter period is that they both underestimate the net longwave radiation. The underestimation of the net longwave radiations takes place because of the overestimation of the upward longwave radiation, and the relative good estimation of the downward longwave radiation. Accordingly, the relative good estimate for the downward longwave radiation occurs due to the cloudless conditions that happens mostly in the winter season [*Walsh and Chapman et al., 1998*]. On the other hand, both reanalyses have problems representing the downward longwave radiation during the spring period. Both ERA-Interim and ERA5 underestimate the downward longwave radiation, which is also seen in [*Bromwich et al., 2015*]. Although, ERA5 has a positive bias at 0.26 $W\ m^{-2}$ that most likely comes from the sudden drop and rise in downward longwave radiation that the ERA5 reanalysis does not notice. The underestimation of the downward longwave radiations likely takes place due to the erroneous cloud representation in the reanalyses. Furthermore, comparing the two reanalyses, ERA5 represents the downward longwave radiation better than does ERA-Interim for this case. In addition, likely die to erroneous clouds conditions in the reanalyses cause an overestimation of the downward shortwave radiation. Thus, the absorption of downward shortwave radiation due to clouds appear to be too small in the use of reanalyses, compared to the real world [*O'Hirok and Gautier et al., 2003*]. On the other hand, the upward shortwave radiation is underestimated in both reanalyses. Accordingly, the underestimation of the upward shortwave radiation indicates that the surface albedo in both ERA-Interim and ERA5 is too low. Similar result for the ERA-Interim reanalysis is found in [*Wesslén et al., 2014*].

At last, both reanalyses represent the mean sea level pressure, the water vapor path and the total wind speed generally well for both periods, concluded from the low biases found in Table 1 and Table 2.

Next, the evaluation on how the assimilated observations from N-ICE2015 influenced the ERA-Interim reanalysis. For this evaluation the probability density functions, mean biases and RMSE values for the difference for the different variables between ERA-Interim and the 12-hour forecast for N-ICE2015 locations and mean of 11 other locations were looked at.

Regarding the result found for the near surface temperature, the result found for the near surface temperature clearly implied that the assimilated temperature observations from N-ICE2015 had influenced the temperature reanalysis data for ERA-Interim. Furthermore, the conclusion for the near surface temperature holds for both winter and spring period. On the

other hand, that the reanalysis is consistently colder than the forecast model temperature after assimilating the N-ICE2015 observations during the whole expedition period could not be confirmed, as was the result in [*Tjernström and Graversen et al., 2009*]. That the reanalysis is consistently colder than the forecast model temperature after assimilating the N-ICE2015 observations were deduced to occur especially during the winter period, because of the negative near surface temperature biases found in Table 3. On the other, positive biases were found for the spring period.

For the mean sea level pressure, it was difficult to deduce if the assimilated observations from N-ICE2015 had an effect on the ERA-Interim reanalysis. For both winter and spring period were the curves in Figure 17 and Figure 18 for both locations somewhat alike. Furthermore, the biases for spring period are quite large, where the other locations had the largest bias. On the other hand, the winter period has reasonably small biases, where the other locations have the smallest bias.

The conclusion for the mean sea level pressure variable is the assimilated N-ICE2015 observations may have had minimal effect on the reanalysis, due to the fact that N-ICE2015 location had relatively better result for the difference between ERA-Interim and 12-hour forecast during spring period. On the other hand, the results from the winter period are consistent with the hypothesis. Thus, the conclusion for the winter period would be that the assimilated N-ICE2015 observations have influenced the reanalysis. Although, for both periods the forecast model may present the mean sea level pressure fairly well.

Already stated in previous section 4.1 the wind speed variable is not assimilated into the reanalysis. Thereby, for the wind speed components the evaluation will focus on to see if the other assimilated observations form N-ICE2015 had an effect on the ERA-Interim reanalysis.

Out from the results for the mean biases and RMSE values for the east-west wind speed the conclusion is that the reanalysis data had been influenced by the assimilation of the N-ICE2015 observations for both winter and spring period. In addition, both periods had small mean biases for the difference between ERA-Interim and 12-hour forecast. Hence, the forecast model can represent the east-west wind speed relatively well, according to [*de Boer et al., 2014*].

The same was concluded for the north-south wind speed, due to the mean biases and RMSE values for the difference between ERA-Interim and 12-hour forecast. On the other hand, the

conclusion can not be made from only looking at Figure 17 and Figure 18, which showed that smaller differences between ERA-Interim and 12-hour forecast occurred more for the N-ICE2015 location.

Finally, the last evaluation that was done in this thesis for finding if the assimilated observations form N-ICE2015 had an effect on the reanalysis ERA5. Examination of the differences between ERA5 reanalysis and the 12-hour forecast were done for this evaluation.

Overall for all variables were the differences between ERA5 and 12-hour forecast smaller, than the differences between ERA-Interim and 12-hour forecast. Moreover, this implies that the forecast model is closer in the ERA5 reanalysis.

The results for the near surface temperature suggest that the assimilated temperature observations from N-ICE2015 have influenced the ERA5 reanalysis value for the near surface temperature. Although, the difference between the two biases from N-ICE2015 and other locations were quite small for both periods, but Figure 19 and Figure 20 showed better results in the differences between ERA5 and 12-hour forecast for the other locations.

Furthermore, the conclusion will also remain for the mean sea level pressure. The assimilated observations from N-ICE2015 have influenced the reanalysis value for the mean sea level pressure. On the other hand, the distinction between N-ICE2015 and other locations were quite small, but still in favour for the other locations. Hence, the assimilated observations from N-ICE2015 have not had quite as large influence on the reanalysis data for mean sea level pressure, compared to the near surface temperature value. Moreover, from the small biases imply that the forecast model simulates the mean sea level pressure remarkably well.

The same conclusion for the mean sea level pressure will apply for the east-west wind speed, due to calculated RMSE values for the east-west wind speed. The RMSE values confirmed the hypothesis, while the biases were contradicted the hypothesis were the difference between the two biases and thus were disregarded. Hence, the east-west wind speed reanalysis variable is slightly affected by the assimilated observation from N-ICE2015.

Furthermore, the same conclusion will apply for the north-south wind speed. In fact, the result for the mean biases and RMSE values for both locations show that the assimilated observations from N-ICE2015 have an effect on the north-south wind speed reanalysis variable from ERA5.

6 Conclusion

Evaluation of the reanalyses in the Arctic region are obviously important, due to the fact that global warming has affected the Arctic climate a great deal. Hence, the thesis focused on the reanalyses ERA-Interim and ERA5, which belongs in the younger generations of reanalyses. The evaluation is particularly important for the ERA5 reanalyses, because it is quite new and few studies have evaluated the ERA5 reanalysis over the Arctic region. Furthermore, the measurements from N-ICE2015 expedition are unique in these field because few other Arctic expedition have measurements particularity for the winter season. In addition, the N-ICE2015 observations were one of the first observations taken over new sea ice condition in the Arctic.

To summaries what the results found for reanalyses performance in section 4.1:

- **WINTER PERIOD**
    - Overestimation of near surface temperature (ERA-Interim better), especially when temperature below -20 ℃.
    - Overestimation of the upward longwave radiation (ERA-Interim better).
    - Underestimation of the net longwave radiation, due to clouds.
    - Good estimates for the mean sea level pressure, water vapor path and the total wind speed.

- **SPRING PERIOD**
    - Still overestimation of near surface temperature and upward longwave radiation, but ERA5 is better when temperature above -3 ℃.
    - Underestimate the downward longwave radiation (ERA5 better).
    - Overestimation of the downward shortwave radiation, due to no cloud in the reanalyses (ERA-I better).
    - Underestimation of the upward shortwave radiation, indicate low surface albedo for both reanalyses (ERA-I better).
    - Good estimates for the mean sea level pressure, water vapor path and the total wind speed.

The overall conclusion is that both reanalyses have insufficient knowledge of the physics in the Arctic climate. The conclusion is a result from the overestimated near surface temperature. In addition, both reanalyses have a to low surface albedo and erroneous cloud parameters, due to the biases found for SWD and SWU.

Table 7 show which of the reanalyses performed best for the variables that were evaluated. The MSLP and the QVI are not in Table 7 because both reanalyses represented these variables quite well.

Table 7: This table show which reanalysis represented the N-ICE2015 observations better. X – better.

Model	**Variable**							
	T2M	**LWD**	**LWU**	**LWN**	**SWD**	**SWU**	**SWN**	**U10M**
ERA-I	X	X	X					
ERA5				X	X	X	X	X

The results from section 4.2 and 4.3 are equally important as the results from section 4.1. The result on if the assimilated observations from N-ICE2015 have an effect on the reanalyses, will imply how inaccurate the reanalyses represent the Arctic when no observations such as those from N-ICE2015 are used in assimilation process for the reanalysis system.

The assimilated N-ICE2015 observations have had an effect on all of the reanalysis variables that were compared for both reanalyses ERA-Interim and ERA5. In addition, the differences between ERA5 and 12-hour forecast were smaller than the differences found for the ERA-Interim reanalysis. The result of this implies that the background forecast model in ERA5 are closer to the observed variables from N-ICE2015, compared to the background forecast model for ERA-Interim.

Bibliography

Barr [1985]. *The Expeditions of the First International Polar Year.* Tech. Paper No. 29. Calgary: Arctic Institute of North America.

Bekryaev, R. V., I. V. Polyakov, and V. A. Alexeev (2010), Role of polar amplification in long-term surface air temperature variations and modern arctic warming, *J. Clim.*, *23*(14), 3888–3906, doi:10.1175/2010JCLI3297.1.

Blunden J, Arndt DS (2012) State of the climate in 2011. *Bull Am Meteorol Soc 93*: S1–S264, Special supplement

Bromwich D. H., A. B. Wilson, L. -S. Bai, G. W. K. Moore, and P. Bauer (2015), A Comparison of the reginal Arctic System Reanalysis and the global ERA-Interim Reanalysis for the Arctic, *Quart. J. Roy. Meteor. Soc., 142*, 644–658, doi:10.1002/qj.2527.

Cassano, J. J., M. E. Higgins, and M. W. Seefeldt (2011), Performance of the Weather Research and Forecasting (WRF) Model for month-long Pan-Arctic simulations, *Mon Weather Rev., 139*, 3469-3488, doi:10.1175/MWR-D-10_05065.1.

CEAREX Drift Group (1990), CEAREX Drift Experiment, *Eos Trans. AGU, 71*(40), 1115–1118, doi:10.1029/90EO00311.

Cesana, G., J. E. Kay, H. Chepfer, J. M. English, and G. de Boer (2012), Ubiquitous low-level liquid-containing Arctic clouds: New observations and climate model constraints from CALIPSO-GOCCP, *Geophys. Res. Lett., 39*, L20804, doi:10.1029/2012GL053385.

Chapman, W. L., and J. E. Walsh (2007), Simulations of Arctic temperature and pressure by Global Coupled Models, *J. Climate, 20*, 609– 632.

Cohen, L., S. R. Hudson, V. P. Walden, R. M. Graham, and M. A. Granskog (2017), Meteorological conditions in a thinner Arctic sea ice regime from winter through early summer during the Norwegian young sea ICE expedition (N-ICE2015), *J. Geophys. Res. Atmos.*, doi:10.1002/2016JD026034.

Comiso, J. C. (2003) Warming Trends in the Arctic from Clear Sky Satellite Observations, *J. Clim., 16*, 3498-3510.

Comiso, J. C., C. L. Parkinson, R. Gersten, and L. Stock (2008), Accelerated decline in the Arctic sea ice cover, *Geophys. Res. Lett., 35*, L01703, doi:10.1029/2007GL031972.

Comiso, J. C. (2012) Large decadal decline of the Arctic multiyear ice cover, *J. Clim., 25*, 1176–1193, doi:10.1175/JCLI-D-11-00113.1.

Cox, C. J., V. P. Walden, and P. M. Rowe (2012), A comparison of the atmospheric conditions at Eureka, Canada, and Barrow, Alaska (2006–2008), *J. Geophys. Res., 117*, D12204, doi:10.1029/2011JD017164.

Dee, D. P., et al. (2011), The ERA-interim reanalysis: Configuration and performance of the data assimilation system, *Q. J. R. Meteorol. Soc., 137*(656), 553–597, doi:10.1002/qj.828.

de Boer G., M. D. Shupe, P. M. Caldwell, S. E. Bauer, O. Persson, J. S. Boyle, M. Kelly, S. A. Klein, and M. Tjernström (2014), Near-surface meteorology during the Arctic Summer Cloud Ocean Study (ASCOS): evaluation of reanalyses and global climate models, *Atmos. Chem. Phys., 14*, doi:10.5194/acp-14-427-2014.

ERA5, European Centre for Medium-Range Weather Forecasts. https://www.ecmwf.int/en/forecasts/datasets/archive-datasets/reanalysis-datasets/era5, 2018. [Online; accessed 01-June-2018].

Francis, J. A., E. Hunter, J. R. Key, and X. Wang (2005), Clues to variability in Arctic minimum sea ice extent, *Geophys. Res. Lett., 32*, L21501, doi:10.1029/2005GL024376.

Gascard, J.-C., et al. (2008), Exploring Arctic transpolar drift during dramatic sea ice retreat, *Eos Trans. AGU, 89*, 21, doi:10.1029/2008EO030001.

Graham, R. M., A. Rinke, L. Cohen, S. R. Hudson, V. P. Walden, M. A. Granskog, W. Dorn, M. Kayser, and M. Maturilli (2017), A comparison of the two Arctic atmospheric winter states during the N-ICE2015 and SHEBA campaigns, *J. Geophys. Res. Atmos., 122*, 5716 –5737, doi:10.1002/ 2016JD025475.

Graversen, R., E. Källén, M. Tjernström and H Körnich (2007), Atmospheric mass-transport inconsistencies in the ERA-40 reanalysis, *Q. J. R. Meteorol. Soc. 133*, 673-680, doi:10.1002/qj.35

Graversen, R. G., and M. Wang (2009), Polar amplification in a coupled climate model with locked albedo, *Clim. Dyn., 33*, 629, doi:10.1007/ s00382-009-0535-6.

Itkin, P., et al. (2017), Thin ice and storms: A case study of sea ice deformation from buoy arrays deployed during N-ICE2015, *J. Geophys. Res. Oceans*, *122*, doi:10.1002/2016JC012403.

Jakobson, E., T. Vihma, T. Palo, L. Jakobson, H. Keernik, and J. Jaagus (2012), Validation of atmospheric reanalyses over the central Arctic Ocean, *Geophys. Res. Lett., 39*, L10802, doi:10.1029/2012GL051591.

Johannessen O. M., E. V. Shalina, M. W. Miled (1999), Satellite Evidence for an Arctic Sea Ice Cover in Transformation, *Science, 286* (5446), 1937-1939, doi:10.1126/science.286.5446.1937.

Kahl, J.D.W., N.A. Zaitseva, V. Khattatov, R. C. Schnell, D.M. Bacon, J. Bacon, V. Radionov, and M.C. Serreze (1999), Radiosonde observations from the former soviet "north pole" series of drifting ice stations, 1954–90, *Bull. Am. Meteorol. Soc., 80,* 2019–2026.

Kalnay, E., et al. (1996), The NCEP/NCAR 40-year reanalysis project, *Bull. Am. Meteorol. Soc., 77,* 437–470.

Kapsch, M. L., R. G. Graversen, T. Economou, and M. Tjernström (2014), The importance of spring atmospheric conditions for predictions of the Arctic summer sea ice extent, *Geophys. Res. Lett., 41,* 5288–5296, doi:10.1002/2014GL060826.

Karlsson, J., and G. Svensson, (2011) The simulation of Arctic clouds and their influence on the winter present-day climate in the CMIP3 multi-model dataset, *Clim. Dynam., 36,* 623–635.

Kay, J. E., and A. Gettelman (2009), Cloud influence on and response to seasonal Arctic sea ice loss, *J. Geophys. Res., 114*, D18204, doi:10.1029/ 2009JD011773.

Kayser, M., M. Maturilli, R. M. Graham, S. R. Hudson, A. Rinke, L. Cohen, J.-H. Kim, S.-J. Park, W. Moon, and M. A. Granskog (2017), Vertical Thermodynamic Structure of the Troposphere during the Norwegian young sea ICE expedition (N-ICE2015), *J. Geophys. Res. Atmos., 122,* doi:10.1002/2016JD026089.

Lindsay, R., M. Wensnahan, A. Schweiger, and J. Zhang (2014), Evaluation of seven different atmospheric reanalysis products in the Arctic, *J. Clim., 27*, 2588–2606, doi:10.1175/JCLI-D-13-00014.1.

Maslanik, J., J. Stroeve, C. Fowler, and W. Emery (2011), Distribution and trends in Arctic sea ice age through spring 2011, *Geophys. Res. Lett. 38*, L13502, doi:10.1029/2011GL047735.

Meyer, A., I. Fer, and A. Sundfjord (2017), Mixing rates and vertical heat fluxes north of Svalbard from Arctic winter to spring, *J. Geophys. Res. Oceans, 122,* doi:10.1002/2016JC012441.

Miller, G. H., R. Alley, J. Brigham-Grette, J. J. Fitzpatrick, L. Polyak, M. C. Serreze, J. W. C. White (2010), Arctic amplification: can the past constrain the fututre? *Quatern. Sci. Rev. 29,* 1779-1790.

Nansen, F. [1898]. *Farthest North*. London: George Newnes, vols. 1 and 2.

Nghiem, S. V., I. G. Rigor, D. K. Perovich, P. Clemente-Colon, J. W. Weatherly, and G. Neumann (2007), Rapid reduction of Arctic perennial sea ice, *Geophys. Res. Lett., 34*, L19504, doi:10.1029/2007GL031138.

O´Hirok W., and C. Gautier (2003), Absorption of shortwave radiation in a cloudy atmosphere: Observed and theoretical estimates during the second Atmospheric Radiation Measurement Enhanced Shortwave Experiment (ARESE), *J. Geophys. Res. 108*, 4412, doi:10.1029/2002JD002818

Onogi, K., and Coauthors, (2007), The JRA-25 Reanalysis, *J. Meteor. Soc. Japan, 85*, 369–432.

Overland, J. E., M. Wang, and S. Salo (2008), The recent arctic warm period, *Tellus A, 60*(4), 589–597.

Park, H. -S., S. Lee, S. -W. Son, S. B. Feldstein, and Y. Kosaka (2015), The impact of poleward moisture and sensible heat flux on Arctic winter sea ice variability, *J. Clim., 28*, 5030–5040, doi:10.1175/JCLI-D-15-0074.1.

Perovich, D. K., et al. (1999), Year on ice gives climate clues, *Eos Trans. AGU, 80*(41), 481–485, doi:10.1029/EO080i041p00481-01.

Perovich, D. K., J. A. Richter-Menge, K. F. Jones, and B. Light (2008), Sunlight, water, and ice: Extreme Arctic sea ice melt during the summer of 2007, *Geophys. Res. Lett., 35*, L11501, doi:10.1029/2008GL034007.

Persson, P. O. G., M. D. Shupe, D. Perovich, and A. Solomon (2016), Linking atmospheric synoptic transport, cloud phase, surface energy fluxes, and sea-ice growth: Observations of midwinter SHEBA conditions, *Clim. Dyn.*, doi:10.1007/s00382-016-3383-1.

Peterson, A. K., I. Fer, M. G. McPhee, and A. Randelhoff (2017), Turbulent heat and momentum fluxes in the upper ocean under Arctic sea ice, J. Geophys. *Res. Oceans, 122*, 1439–1456, doi:10.1002/2016JC012283.

Pithan, F., B. Medeiros, and T. Mauritsen (2014), Mixed-phase clouds cause climate model biases in Arctic winter time temperature inversions, *Clim. Dyn., 43*(1–2), 289–303, doi:10.1007/s00382-013-1964-9.

Polyakov I.V., J. E. Walsh, R. Kwok (2012), Recent changes of Arctic multiyear sea ice coverage and the likely causes. *Bull Am Meteorol Soc 93*:145–151.

Raddatz, R. L., T. N. Papakyriakou, B. G. Else, M. G. Asplin, L. M. Candlish, R. J. Galley, and D. G. Barber (2015), Downwelling longwave radiation and atmospheric winter

states in the western maritime Arctic, *Int. J. Climatol., 35*(9), 2339–2351, doi:10.1002/joc.4149.

Russian North Pole drifting station program, https://arctic.ru/geographics/20180219/719368.html, 2018. [Online; access: 25-May-2018]

Serreze, M. C., and R. G. Barry (2011), Processes and impacts of arctic amplification: A research synthesis, *Global Planet. Change, 77*, 85 –96.

Serreze, M. C. and R. G. Barry [2014]. *The Arctic Climate System (Second Edition)*. Cambrigde University Press. 1, 11-22.

Simmons A. J, and P. Poli (2015), Arctic warming in ERA-Interim and other analyses, *Q. J. R. Meterorol. Soc., 141*, 1147-1162, doi:10.1002/qj-2422.

Solomon S., D. Qin, M. Manning, Z. Chen, M. Marquis, K. Averyt, M. Tignot, and H. Miller (2007) Climate change 2007: the physical science basis. *Cambridge University Press*, Cambridge.

Sotiropoulou, G., J. Sedlar, R. Forbes, and M. Tjernström (2015), Summer Arctic clouds in the ECMWF forecast model: An evaluation of cloud parametrization schemes, *Q. J. R. Meteorol. Soc., 142*, 387–400, doi:10.1002/qj.2658.

Stramler, K., A. D. Del Genio, and W. B. Rossow (2011), Synoptically driven Arctic winter states, *J. Clim., 24*(6), 1747–1762, doi:10.1175/ 2010JCLI3817.1

Stroeve, J. C., T. Markus, L. Boisvert, J. Miller, and A. Barrett (2014), Changes in Arctic melt season and implications for sea ice loss, *Geophys. Res. Lett., 41*, 1216–1225, doi:10.1002/2013GL058951.

Tjernström, M., et al. (2012), Meteorological conditions in the central Arctic summer during the Arctic Summer Cloud Ocean Study (ASCOS), *Atmos. Chem. Phys., 12*(15), 6863–6889, doi:10.5194/acp-12-6863-2012.

Tjernström, M., C. Leck, C. E. Birch, B. J. Brooks, I. M. Brooks, L. Bäcklin, R. Y.-W. Chang, E. Granath, M. Graus, A. Hansel, J. Heintzenberg, A. Held, A. Hind, S. de la Rosa, P. Johnston, J. Knulst, G. de Leeuw, L. Di Liberto, M. Martin, P. A. Matrai, T. Mauritsen, M. Müller, S. J. Norris, M. V. Orellana, D. A. Orsini, J. Paatero, P. O. G. Persson, Q. Gao, C. Rauschenberg, Z. Ristovski, J. Sedlar, M. D. Shupe, B. Sierau, A. Sirevaag, S. Sjogren, O. Stetzer, E. Swietlicki, M. Szczodrak, P. Vaattovaara, N. Wahlberg, M. Westberg, C. R. and Wheeler (2013), The Arctic Summer Cloud-Ocean Study (ASCOS): overview and experimental design, *Atmos. Chem. Phys. Discuss., 13*, 13541– 13652, doi:10.5194/acpd-13-13541-2013.

Tjernström, M., and R. G. Graversen (2009), The vertical structure of the lower Arctic troposphere analysed from observations and the ERA-40 reanalysis, Q. J. R. *Meteorol. Soc., 133*, 937–948, doi:10.1002/qj.380.

Uppala S. M., P. W. Kållberg, A. J. Simmons, U. Andrae, V. Da Costa Bechtold, M. Fiorino, J. K. Gibson, J. Haseler, A. Hernandez, G. A. Kelly, X. Li, K. Onogi, S. Saarinen, N. Sokka, R. P. Allan, E. Andersson, K. Arpe, M. A. Balmaseda, A. C. M. Beljaars, L. Van de Berg, J. Bidlot, N. Bormann, S. Caires, F. Chevallier, A. Dethof, M. Dragosavac, M. Fisher, M. Fuentes, S. Hagemann, E. Hólm, B. J. Hoskins, L. Isaksen, P. A. E. M. Janssen, R. Jenne, A. P. McNally, J. -F. Mahfouf, J. -J. Morcrette, N. A. Rayner, R. W. Saunders, P. Simon, A. Sterl, K. E Trenberth, A. Untch, D. Vasiljevic, P. Viterbo, J. Woollen (2005), The ERA-40 re-analysis. *Q. J. R. Meteorol. Soc. 131*: 2961–3012.

Vihma, T., J. Jaagus, E. Jakobson, and T. Palo (2008), Meteorological conditions in the Arctic Ocean in spring and summer 2007 as recorded on the drifting ice station Tara, *Geophys. Res. Lett., 35*, L18706, doi:10.1029/2008GL034681.

Vihma T. (2014), Effects of Arctic Sea Ice Decline on Weather and Climate: A Review, *Surv Geophys 35*, 1175-1214, doi:10.1007/s10712-014-9284-0.

Walsh, J. E., V. M. Kattsov, W. L. Chapman, V. Govorkova, and T. Pavlova (2002), Comparison of Arctic climate simulations by uncoupled and coupled global models, *J. Climate, 15*, 1429–1446.

Walsh, J. E., and W. L. Chapman (1998), Arctic cloud–radiation–temperature associations in observational data and atmospheric reanalyses, *J. Clim., 11*, 3030–3045, doi:10.1175/1520-0442(1998)011<3030:ACRTAI>2.0. CO;2.

Wesslén, C., M. Tjernström, D. H. Bromwich, G. de Boer, A. M. L. Ekman, L.-S. Bai, and S.-H. Wang (2014), The Arctic summer atmosphere: An evaluation of reanalyses using ASCOS data, *Atmos. Chem. Phys., 14*, 2605–2624, doi:10.5194/acp-14-2605-2014.

Wilson, A. B., D. H. Bromwich, and K. M. Hines (2011), Evaluation of Polar WRF forecasts on the Arctic System Reanalysis domain: Surface and upper air analysis, *J. Geophys. Res., 116*, D11112, doi:10.1029/2010JD01501.

Woods, C., R. Caballero, and G. Svensson (2013), Large-scale circulation associated with moisture intrusions into the Arctic during winter, *Geophys. Res. Lett., 40*, 4717–4721, doi:10.1002/grl.50912.

Wyser, K., et al. (2008), An evaluation of Arctic cloud and radiation processes during the SHEBA year: Simulation results from eight Arctic regional climate models, *Clim. Dyn., 30*, 203, doi:10.1007/s00382-007-0286-1

Zhang, J., R. Lindsay, M. Steele, and A. Schweiger (2008), What drove the dramatic retreat of arctic sea ice during summer 2007?, *Geophys. Res. Lett.*, *35*, L11505, doi:10.1029/2008GL034005.